



كلية الدراسات العليا

Sudan University of Science & Technology

College Graduate Studies



**The Effect of Changing Solvent, Dyes and ZnO Nanosize On The
Performance of ZnO Solar Cell**

تأثير تغيير المذيبات والصبغات واكسيد الزنك النانوي علي أداء خلية أكسيدالزنك الشمسية

**A Dissertation submitted in partial fulfillment for the Degree of
Doctor of Philosophy in physics**

By

Asia GamarEldawla EL-Tayeb Abdelmagid

Supervisor

Professor Mubarak Dirar Abd-alla

February- 2020

بِسْمِ اللَّهِ الرَّحْمَنِ الرَّحِيمِ

الآية

قال تعالى:

(يُبَيِّنُ إِنَّهَا إِنْ تَكُ مِثْقَالَ حَبَّةٍ مِنْ خَرْدَلٍ فَتَكُنْ فِي صَخْرَةٍ أَوْ فِي السَّمَوَاتِ أَوْ فِي
الْأَرْضِ يَأْتِ بِهَا اللَّهُ إِنَّ اللَّهَ لَطِيفٌ خَبِيرٌ)

صدق الله العظيم [لقمان:16].

Dedication

To my dear ; Dear father ;I owe you this. To my brothers; professors , colleagues comrades of the trail, and to those who loved me honestly; and I love them equally.

Acknowledgements

Thanks first to Allah, and especial thanks to my professor . Mubarak Dirar Abd-alla ,and thanks goes to my family supported me to finish this work, a thank Mr Abdalsakhi Soliman .M.H. the family college of science, physics and chemistry department, and also Thanks to the Dr.Mohammed Idriss Ahmad of Sudan Atomic Energy Commission, family of ELNeenlen University department of chemistry, my friend Tawsol eltayeb mohamud , Thanks also for each of the financially or cognitively contributed to the completion of this research modest.

Abstract

The effect of different solvents on Zinc Oxide based Dye Sensitized Solar Cells (DSSC) with Nile Blue were studied. The performance of solar cells with on (FTO/ ZnO/ Blue Nile dye /FTO+ graphite and Iodine) structures were investigated under the effect of different solvents, which on (Methanol ,Ethanol ,Acton , Chloroform and Benzene). Absorption and energy gap were found using UV-VS mini 1240 spectrophotometer and light current-voltage characteristics and XRD. The five (FTO/ ZnO/ Blue Nile dye /FTO+ graphite) solar cells were produced and characterized. provided efficiency (η) were (0.40165,0.3968 ,0.3858 ,0.3719 and 0.3477).which decrease when the absorbance decreases taking values(Methanol = (2.005 a.u) ,Ethanol = (1.4819 a.u) ,Acton = (1.221 a.u) , Chloroform = (0.983 a.u) and Benzene = (0.532 a.u)). The decrease of efficiency due to absorbance decreasing may be attributed to the decrease of atoms density which decreases with the Nano crystal size.

Zinc Oxide based Dye Sensitized Solar Cells (DSSC) with Rose Bengal were fabricated also on FTO glass .The five solvents used were (Methanol ,Ethanol ,Acton, Chloroform and Benzene). Microstructure and cell performance of the solar cells with (FTO/ ZnO/ Rose Bengal dye /FTO+ graphite and Iodine) structures were investigated taking into account the effect of solvents. Photovoltaic devices based on the ZnO/ Rose Bengal dye hetrojunction structures provided photovoltaic properties under illumination. Absorption and energy gap measurement of the ZnO/ Rose Bengal dye hetrojunction were studied using UV-VS mini 1240 spectrophotometer and light current-voltage characteristics an XRD. The energy gaps of the present solar cells were also found. The five (FTO/ ZnO/ Rose Bengal dye /FTO+ graphite) solar cells were produced and characterized, which provided efficiency (η) and Energy gap (0.6795 for $E_g = 2.947$ eV ,0.63901

for $E_g = 2.951$ eV ,0.58821for $E_g = 2.958$ eV ,0.55262 for $E_g = 2.963$ eV and 0.50864 for $E_g = 2.972$ eV) Fill factor (FF) average (0.89) for all cells . This means that the increase of energy gap value decreases efficiency. It was also found that the increase of absorbance and distance between Nano crystal increases the efficiency.

المستخلص

تمت دراسة تأثير مذيبيات مختلفة علي الخلية الشمسية الصبغية المعتمده علي اوكسيد الزنك (FTO/ ZnO/ Blue Nile dye) للصبغة النيلية الزرقاء. وتمت مناقشة ودراسة أداء الخلايا (FTO+ graphite and Iodine) الميثانول و الايثانول ،الاستون) والكوروفورم والبنزين). تم ايجاد فجوة الطاقة و الامتصاصية باستخدام مطياف الاشعة فوق البنفسجية والمرئية الصغيرة بالرقم ١٢٤٠ مع الخواص الضوئية والتيارية والجهدية وجهاز حيود اشعة X.

(FTO/ ZnO/ Blue Nile dye /FTO+ graphite and Iodine) صنفت الخمس خلايا شمسية (الفلورين واكسيد الزنك /الصبغة النيلية الزرقاء/الفلورين واكسيد الزنك والجرافيت 0.3719, 0.3858, 0.3968, 0.40165) والايودين) ودرست خصائصها. حيث كانت كفاءتها (0.3719, 0.3858, 0.3968, 0.40165) تنقص بنقصان الامتصاص الذي ياخذ القيم (0.3477 and 0.3719). ويعزي نقصان الكفاءة بسبب الامتصاص وذلك لنقصان كثافة الذرات التي تقل (0.3477 and 0.3719) مع البعد النانوي البلوري. وصنفت ايضاً خلايا شمسية صبغية معتمدة علي اوكسيد الزنك لصبغة الروز البنغاليه علي زجاج الفلورين (FTO). وكانت المذيبيات الخمسة المستخدمة هي) الميثانول والايثانول والاستون والكوروفورم والبنزين). تمت مناقشة التركيب الدقيق واداء (FTO/ ZnO/ .Rose Bengal dye /FTO+ graphite and Iodine) الخلية. للخلايا الشمسية مع الاخذ في الاعتبار تأثير المذيبيات. هذه الاجهزه الفوتوفولطائية المعتمدة علي اوكسيد الزنك وصبغة روز البنغاليه ذو الملتقيات المتعددة لتظهر خواص كهروضوئية بتاثير الاضاءة. درست الامتصاصية وفجوة الطاقة واخذت القراءات لملتي اوكسيد الزنك وصبغة روز البنغاليه باستخدام جهاز مطياف الاشعة فوق البنفسجية والمرئية الصغيرة رقم ١٢٤٠ بالإضافة للخواص الضوئية والتيارية والجهدية وجهاز حيود اشعة X. وتم ايضاً ايجاد فجوة الطاقة لهذه الخلايا الشمسية. تم تصنيع ودراسة خصائص الخمس (FTO/ ZnO/ Rose .Bengal dye /FTO+ graphite and Iodine) خلايا شمسية مصنعة من

وقد كانت كفاءتها وفجوة طاقاتها هي (0.6795 % for $E_g = 2.947$ eV ,0.63901 % for $E_g = 2.951$ eV ,0.58821% for $E_g = 2.958$ eV .,0.55262 % for $E_g = 2.963$ eV and 0.50864 % for $E_g = 2.972$ eV) وهذا . وكان متوسط عامل الملء هو 0.89 لكل الخلايا . يعني ان زيادة قيمة فجوة الطاقة تقلل من الكفاءة. ووجد ايضاً ان زياده الامتصاصية والمسافة بين البلورات النانوية تزيد الكفاءة.

Abbreviations	Terminology
DSC(s)	Dye-sensitized solar cells
DSSC	dye-sensitized solar cells
ZnO	Zinc oxide
FTO	Fluorescein tin oxide
ITO	Indium tin oxide
TCO	Transparent conducting oxide
NC(s)	Nanocrystal (s)
TiO ₂	Titanium dioxide
FWHM	Full width at half maximum
XSCs	Excitonic solar cells
OSCs	organic solar cells
HSCs	hybrid organic/inorganic solar cells
P3HT	poly(3-hexylthiophene)
CBD	chemical bath deposition
ALD	atomic layer deposition
VLS	vapour-liquid-solid
MOCVD	metal-organic chemical vapor deposition
AUST	African University of Science and Technology
MRSP	mirror reflected solar panel
all-PSCs	All –polymer solar cells
NDI	naphthalene dioxide
LUMO	lowest unoccupied molecular orbital
PCE	power conversion efficiency
SEM	scanning electron microscopy
FTIR	Fourier transformed infrared spectroscopy
TEM	transmission electron microscopy
XRD	X-ray powder diffractometry

List of Figures

Figure No.	Title	Page No.
2.1	Schematic of concentrated solar cells	8
2.2	Various types of solar cell technologies and current trends of development	9
2.3	FTO glass	14
4.1	heat the solution to 60°C under continuous stirring	52
4.2	The solution transparent	52
4.3	FTO glass fixed on the board	53
4.4	Deposition of ZnO nanoparticle onto FTO glass	54
4.5	schematic structure of (FTO/ ZnO/ Blue Nile dye /FTO+ graphite and Iodine	55
4.6	Nile blue dye with (Methanol, Ethanol, Acton, Chloroform and Benzene)	56
4.7	Reading (I, V) for solar cell with Nile blue	56
4.8	schematic structure of (FTO/ ZnO/ Rose Bengal /FTO+ graphite and Iodine)	58
4.9	Bengal rose dye with (Methanol, Ethanol, Acton, Chloroform and Benzene)	58
4.10	Reading (I, V) for solar cell with Bengal rose The samples ready for characterization.	59
4.11	SEM image of ZnO	59
4.12	XRD spectrum of Nano ZnO sample	60
4.13	EDS spectra of the ZnO nano sample	61
4.14	relation between Absorption Coefficient (α) and wavelengths of ZnO sample	62
4.15	Optical Energy Band Gap of ZnO sample	62
4.16	relation between absorbance and wavelengths of five sample that made by Blue Nile dye in different solvent (Methanol ,Ethanol ,Acton m Chloroform	63

	and Benzene)	
4.17	relation between absorption coefficient and wavelengths of five sample that made by Blue Nile dye in different solvent (Methanol ,Ethanol ,Acton m Chloroform and Benzene)	64
4.18	The optical energy band gab of five sample that made by Blue Nile dye in different solvent (Methanol ,Ethanol ,Acton m Chloroform and Benzene)	65
4.19	several factors for characterization of Nile Blue with Methanol solar cell	66
4.20	several factors for characterization of Nile Blue with Ethanol solar cell	66
4.21	several factors for characterization of Nile Blue with Acton solar cell	67
4.22	several factors for characterization of Nile Blue with Chloroform solar cell	68
4.23	several factors for characterization of Nile Blue with Benzene solar cell	68
4.24	The relationship between Absorbance and efficiency of Dye Sensitized Solar Cells (DSSC) by (ZnO+ Nile Blue dye) samples.	70
4.25	Relationship between energy band gap and efficiency of Dye Sensitized Solar Cells (DSSC) by (ZnO+ Nile Blue dye) samples	71
4.26	Relationship Between efficiency and Density of Dye Sensitized Solar Cells (DSSC) by (ZnO+ Nile Blue dye) samples	71
4.27	Relation between absorbance and wavelengths of five sample that made by Rose Bengal dye in different solvent(Methanol, Ethanol, Acton, Chloroform and Benzene	72
4.28	Relation between absorption coefficient and wavelengths of five sample that made by Rose Bangal dye in different solvent (Methanol ,Ethanol	73

	,Acton m Chloroform and Benzene)	
4.29	The optical energy band gab of five sample that made by Rose Bengal dye in different solvent (Methanol ,Ethanol ,Acton Chloroform and Benzene)	74
4.30	several factors for characterization of Rose Bangal with Methanol solar cell	75
4.31	several factors for characterization of Rose Bangal with Ethanol solar cell	75
4.32	several factors for characterization of Rose Bangal with Acton solar cell	76
4.33	several factors for characterization of Rose Bangal with Chloroform solar cell	76
4.34	several factors for characterization of Rose Bangal with Benzene solar cell	77
4.35	The relationship between Absorbance and efficiency of Dye Sensitized Solar Cells (DSSC) (ZnO+ Rose Bengal dye dye)samples	77
4.36	The relationship between Energy band gap and efficiency of Dye Sensitized Solar Cells (DSSC) (ZnO+ Rose Bengal dye dye) samples)	79
4.37	The relationship between Energy band gap and efficiency of Dye Sensitized Solar Cells (DSSC) (ZnO+ Rose Bengal dye dye) samples	80
4.38	The relationship between Density Current and efficiency of Dye Sensitized Solar Cells (DSSC) (ZnO+ Rose Bengal dye dye) samples	80

List of Table

2.1	Absorption λ max(nm) and Emission λ max (nm) for solvent	29
2.2	Physical Properties of Solvents	29
4.1	Lattice Constants from Peak Locations and Miller Indices [Cubic - F-center] of ZnO sample	59
4.2	Calculate Lattice Constants from Peak Locations and Miller Indices [Cubic _ F-center] of ZnO sample	63
4.3	Typical I-V riding of Nile Blue with Methanol solar cell	65
4.4	Typical I-V riding of Nile Blue with Ethanol solar cell	65
4.5	Typical I-V riding of Nile Blue with Acton solar cell	66
4.6	Typical I-V riding of Nile Blue with Chloroform solar cell	67
4.7	Typical I-V riding of Nile Blue with Benzene solar cell	67
4.8	Typical I-V riding of five sample that made by Blue Nile dye in different solvent (Methanol ,Ethanol ,Acton m Chloroform and Benzene)	69
4.9	Lattice Constants and Miller Indices [Cubic Face centered] of ZnO sample	72
4.10	Typical I-V riding of Rose Bangal with Methanol solar cell	73
4.11	Typical I-V riding of Rose Bangal with Ethanol solar cell	73

4.12	Typical I-V riding of Rose Bangal with Acton solar cell	71
4.13	Typical I-V riding of Rose Bangal with Chloroform solar cell	72
2.14	Typical I-V riding of Rose Bangal with Benzene solar cell	72
2.13	Typical I-V riding of five sample that made by Rose Bangal dye in different solvent (Methanol ,Ethanol ,Acton m Chloroform and Benzene)	75
4.15	Typical I-V riding of five sample that made by Rose Bangal dye in different solvent (Methanol ,Ethanol ,Acton m Chloroform and Benzene)	77

List of Contents

Subject	Page No.
الآية	I
Dedication	II
Acknowledgements	III
Abstract	IV
الخلاصة	V
List of Figures	VI
List of Tables	VII
Table of contents	VIII-X

Figure No.	Title	Page No.
	Chapter one	
1.1	Energy and Physics	1
1.3	Research problem	4
1.4	Aim of this work	4
1.5	Thesis layout	4
	Chapter tow	
2.1	Introduction	5
2.2	Solar Cells	5
2.3	First Generation Solar Cell	6
2.4	Second Generation Solar Cells—Thin Film Solar Cells	6
2.5	Third Generation Solar Cells	6
2.6	Concentrated Solar Cells	7
2.7	Various types of solar cell technologies and current trends of development	8
2.8	The Potential of Photovoltaic	9
2.9	Dye Sensitized Solar Cells (DSSC)	10
2.10	THE advanced fluorescent concentrator concept	11
2.11	Substrates	12
2.12	FTO glass	12
2.12.1	Fluorine doped Tin Oxide (FTO) glass	13
2.12.2	Features and benefits of FTO	13
2.13	ZnO nanostructures	14
2.13.1	Electrical properties	15
2.14	Facile synthesis of ZnO nanoparticle on FTO glass for dye-sensitized solar cells	16
2.15	Dyes	17
2.15.1	Types of dyes	17
215.1.1	Inorganic dye	17
2.15.1.2	Organic dye	17

2.15.1.3	Natural dyes	19
2.16	Organic complex of other metals	19
2.17	Rose Bengal	19
2.17.1	History and etymology	20
2.17.2	Chemical applications	20
2.18	Nile blue	19
2.18.1	Chemical and physical properties	20
2.19	Solvent	20
2.19.1	Physical Properties of Solvents	20
2.20	Oxides	21
2.21	Oxides of Precious Metals	22
2.22	Oxides of Fusible Metals	22
2.23	Oxides in Contemporary Photovoltaic Cell Technologies	23
2.24	Ideal Material Characteristics for Various Functions in PV Cells	24
2.25	High Efficiency Concepts	25
2.26	Efficiency limitations	26
2.27	Background on Hybrid Photovoltaic	26
2.28	Characterizing performance of solar cells	27
	Chapter three	
3.1	Introduction	29
3.2	A study on the reliability and performance of solar powered street lighting systems	29
3.3	A Review Paper on Electricity Generation from Solar Energy	30
3.4	Performance Comparison of Mirror Reflected Solar Panel with Tracking and Cooling	30
3.5	High Voltage All Polymer Solar Cells with a Polymer Acceptor based on NDI and Benzotriazole	32
3.6	Comprehensive Study on Chemical and Hot Press-Treated Silver Nanowires for Efficient Polymer Solar Cell Application	33

3.7	Synthesis and characterization of zinc oxide nanoparticles: application to textiles as UV-absorbers	34
3.8	Fully Printed Zinc Oxide Electrolyte-Gated Transistors on Paper	34
3.9	Functional behavior of paper coated with zinc oxide – soluble starch Nano composites	35
3.10	Nano-Photonic Structures for Light Trapping in Ultra-Thin Crystalline Silicon Solar Cells	36
3.11	High Efficiency Silicon Solar Cell	37
3.12	Fabrication and Characterization of Rose Bengal Sensitized Binary TiO ₂ -ZrO ₂ Oxides Photo-electrode Based Dye-sensitized Solar Cells	38
3.13	Preparation of Fluorine-doped Tin Oxide by a Spray Pyrolysis Deposition and Its Application to the fabrication of Dye-sensitized Solar Cell Module	38
3.14	Solar cells based on synthesized nanocrystalline ZnO thin films sensitized by chlorophyll a and photopigments isolated from spinach	39
3.15	Facile synthesis of ZnO nanowires on FTO glass for dye-sensitized solar cells	40
3.16	Comparison of transparent conductive indium tin oxide, antimony-doped indium oxide, and fluorine-doped tin oxide films for dye-sensitized solar cell application	41
3.17	Using Gum Arabic in Making Solar Cells by Thin Films instead Of Polymers	41
3.18	Applications of Oxide Coatings in Photovoltaic Devices	42
3.19	Electro deposition of In ₂ S ₃ Thin Films onto FTO Substrate from DMSO Solution	44
3.20	Polymeric Materials for Conversion of Electromagnetic Waves from the Sun to Electric Power	45
3.21	Rational Design of Solar Cells for Efficient Solar Energy Conversion	46

3.22	Photovoltaic Effect on Molecule Couple Ferromagnetic Films of a Magnetic Tunnel Junction	47
3.23	Fabrication and characterization of vacuum deposited fluorescein thin films	47
3.24	Recent trends on nanostructures based solar energy applications	49
Chapter four		
4.1	Introduction	50
4.2	Materials and Equipment's	51
4.3	Methodology	51
4.3.1	ZnO preparation	51
4.3.2	The aqueous chemical growth solution	52
4.4	Methodology for solar cell	53
4.4.1	Materials and Methods for Nile Blue	54
4.4.2	Materials and Methods for Rose Bengal	56
4.5	Results and Discussion for ZnO	59
4.6	Dye Blue Nile Results and Discussion	63
4.7	Blue Nile Solar Cell Results and Discussion	65
4.8	Dye Rose Bengal Results and Discussion	71
4.9	Rose Bengal Solar Cell Results and Discussion	73
Chapter five		
Conclusion and Recommendation		
5.1	for Nile blue	80
5.2	Conclusion for Rose Bengal	80
5.3	Recommendation	80
5.4	Future work	81
References		

Chapter One

Introduction

1.1 Energy and Physics

Fuel energy is very essential for people. Consumption and excessive greenhouse gas emissions have put significant pressure on energy needs for human life. The growing need for energy can be met by solar cell technology. The solar cell technology has not been in large-scale utilization because of its high cost and insufficient conversion efficiencies. Fortunately recent researches in nanomaterial and device technologies have offered new opportunities for it to become competitive to fossil fuels. Among various photovoltaic devices, the excitonic solar cells (XSCs) technology has made enormous progresses and is highly competitive for large SC commercial fabrication. The aim of the research on XSCs is to develop photovoltaic technology which allows solar cells to be produced on flexible substrate by using high throughput roll-to-roll method at low cost. Ideally, all of the fabrication process could be done using low-temperature, low power-consumption, low cost, and solution-based process. This dissertation follows the style of Nanotechnology.

In XSCs, conjugated polymers, small molecules, or quantum dots are utilized as the light absorbing materials. Upon light absorption, excitations (bound electron-hole pairs) are generated. If they are not formed at the interface between constituent semiconductors, it is necessary for these excitations to diffuse to the interface without recombination. So long as the offset of energy levels at the junction is greater than the exciton binding energy, free charge carriers can be created [1,3]. For this reason, the majority of the carriers are present at the interface and the interfacial property becomes crucial. In addition, excitation diffusion length also has a significant impact on the performance of XSCs. Only

those exactions generated within the order of the exaction diffusion length from the interface have chances to reach interface and separate into free charges. In other words, it is beneficial to fabricate excitonic devices with interface everywhere in the material. For conductive polymers, diffusion length ranges from 4 nm to 20 nm [4] for high quality small molecule thin films, it's up to a micrometer [5]. Oppositely, in conventional photovoltaic devices, free electron-hole pairs are produced everywhere in the bulk semiconductor and subsequently separate when they arrive at the junction. Therefore, the charge generation and separation are different between XSCs and conventional solar cells and result in fundamental difference in device behavior. Excitonic photovoltaic devices include organic solar cells (OSCs), hybrid organic/inorganic solar cells (HSCs), and dye-sensitized solar cells (DSSCs). The most efficient XSCs reported are Grätzel's DSSCs with efficiencies of 11% [6, 8]. Despite the high efficiency, DSSCs based on liquid electrolyte have reliability issues caused by the liquid redox electrolyte. Device instability and the need for good device packaging have become major hurdles for commercial application of DSSCs [9]. Furthermore, liquid electrolyte based solar cells cannot be easily fabricated into multi-cell modules [10]. One way to address this manufacturing difficulty is to replace the liquid redox electrolyte by a solid-state hole transport material, typically a p-type conjugated polymer. Recently, many attempts have been made by using different hole transport materials, such as OMeTAD [11,12], and poly(3-hexylthiophene) (P3HT) [13], along with dye-loaded porous nanoparticle films. Efficiencies of solid-state DSSCs remain around 4% [14]. Recent progresses in nanotechnologies have led to improved efficiency in OSCs from planar p-n junction cells to bulk heterojunction cells with efficiencies up to 5-7% [15, 18].

By modifying the morphology of inorganic constituent in HSCs and DSSCs, the photovoltaic efficiency could be improved. As the key components, many

inorganic semiconductors have been applied as nanostructured materials for XSCs, such as TiO_2 , ZnO , CdSe , PbS , CuInSe , and many others. Among these electron transport materials, ZnO is an attractive candidate because of its diverse morphologies. ZnO is a II-VI binary compound semiconductor with a large band gap of 3.2 eV, and the conduction band edge of ZnO is at -4.4 V versus vacuum [19]. As a direct and wide band gap material, it draws a lot of interests as the candidate for electronic and short wavelength optoelectronic applications. ZnO has a diverse group of nanostructures, for instance, nanoparticles, nanorods, vertically aligned Nano rods/nanowires, core-shell nanorods/nanowires, nanotubes, nenobelts, nanosheets, nanoflowers, hierarchical structures, and branched structures. These nanostructures can be synthesized through sol gel synthesis, hydrothermal growth, chemical bath deposition (CBD), atomic layer deposition (ALD), vapour-liquid-solid (VLS) approach, or metal-organic chemical vapor deposition (MOCVD). The reduction of the structures to Nano scale provides novel electrical, mechanical, and optical properties as the result of surface and quantum confinement effects. Though power conversion efficiency of solar cells based on ZnO is lower than that of TiO_2 , ZnO is still regarded as a prominent competitor due to its ease of synthesis and flexibility on the nanostructure morphologies. In addition, the electron mobility of ZnO is higher than that of TiO_2 , the charge recombination rate of ZnO is lower than that of TiO_2 , and the electron lifetime of ZnO is longer than that of TiO_2 . Those characteristics are beneficial for solar cell applications.

1.2 Research problem

Fuel energy causes several biological hazards. Fuel capacity is also limited and environmental pollution. This needs pollution free, sustainable, energy resource. Although solar energy appear to be best candidate, but solar cells, that are more popular solar conversions, have low efficiency and high cost.

1.3 Aim of this work:

The aim of this work is the Preparation of ZnO Nanoparticle by using different solvents so as to fabricate solar cells. The effect of these solvent on the Nano ZnO structure is also investigated.

1.4 Thesis layout

The thesis consists of five chapters. Chapter one is introduction, while chapter Two concerned with the theoretical background. The Literature Review is in chapter Three. The materials and methods are in chapter Four. The discussion and conclusion are in chapter Five.

Chapter Two

Theoretical Background

2.1 Introduction

This chapter covers the physics needed to understand the performance of a high efficiency solar cell. What is needed is how to increase the photocurrent conversion efficiency. In recent years, research into high-efficiency solar cells has accelerated with the rapid emergence of new materials and devices showing promising performance characteristics. To increase the photocurrent conversion efficiency, it is necessary to choose a suitable material, fabricate a device with proper structure, and to understand the physics behind the materials. This chapter is devoted for the physics of the solar cells.

2.2 Solar Cells

The radiation electricity conversion named photovoltaic (PV) effect was first observed by Alexandre-Edmond Becquerel in 1839. Subsequently, in 1946 the first modern solar cell made of silicon was invented by Russel Ohl [20,21]. The modern photovoltaic technology is based on the principle of electron hole creation in each cell composed of two different layers (p-type and n-type materials) of a semiconductor material. In this cell, when a photon of sufficient energy impinges on the p-type and n-type junction, an electron is ejected by gaining energy from the striking photon and moves from one layer to another. This creates an electron and a hole in the process and by this process electrical power is generated [22]. The various types of materials applied for photovoltaic solar cells includes mainly in the form of silicon (single crystal, multi-crystalline, amorphous silicon) [23,24], cadmium-telluride [25], copper-indium-gallium-selenite [26], and copper-indium-gallium-sulfide [27].

2.3 First Generation Solar Cell

The first generation solar cells are produced on silicon wafers. It is the oldest and the most popular technology due to high power efficiencies. The silicon wafer based technology is further categorized into two subgroups named as [28,29].

- Single/ Mono-crystalline silicon solar cell.
- Poly/Multi-crystalline silicon solar cell.

2.4 Second Generation Solar Cells—Thin Film Solar Cells

Most of the thin film solar cells and a-Si are second generation solar cells, and are more economical as compared to the first generation silicon wafer solar cells. Silicon-wafer cells have light absorbing layers up to 350 μ m thick, while thin-film solar cells have a very thin light absorbing layers, generally of the order of 1 μ m thickness [30]. Thin film solar cells are classified as;

- a-Si.
- CdTe.
- CIGS (copper indium gallium di-selenide).

2.5 Third Generation Solar Cells

Third generation cells are the new promising technologies but are not commercially investigated in detail. Most of the developed 3rd generation solar cell types are [31]:

- 1) Nano crystal based solar cells.
- 2) Polymer based solar cells.
- 3) Dye sensitized solar cells.

4) Concentrated solar cells

2.6 Concentrated Solar Cell

Concentrating photovoltaic (CPV) has been established since the 1970s [32, 33, 34]. It is the newest technology in the solar cell research and development. The main principle of concentrated cells is to collect a large Amount of solar energy onto a tiny region over the PV solar cell, as shown in Figure 2.1. The principle of this technology is based on optics, by using large mirrors and lens arrangement to focus sunlight rays onto a small region on the solar cell [35]. The converging of the sunlight radiations thus produces a large amount of heat energy. This heat energy is further driven by a heat engine controlled by a power generator with integrated. CPVs have shown their promising nature in solar world [36] [37]. It can be classified into low, medium, and high concentrated solar cells depending on the power of the lens systems [38]. Concentrating photovoltaic technology have the following merits, such as solar cell efficiencies >40%, absence of any moving parts, no them mass, speedy response time and can be scalable to a range of sizes.

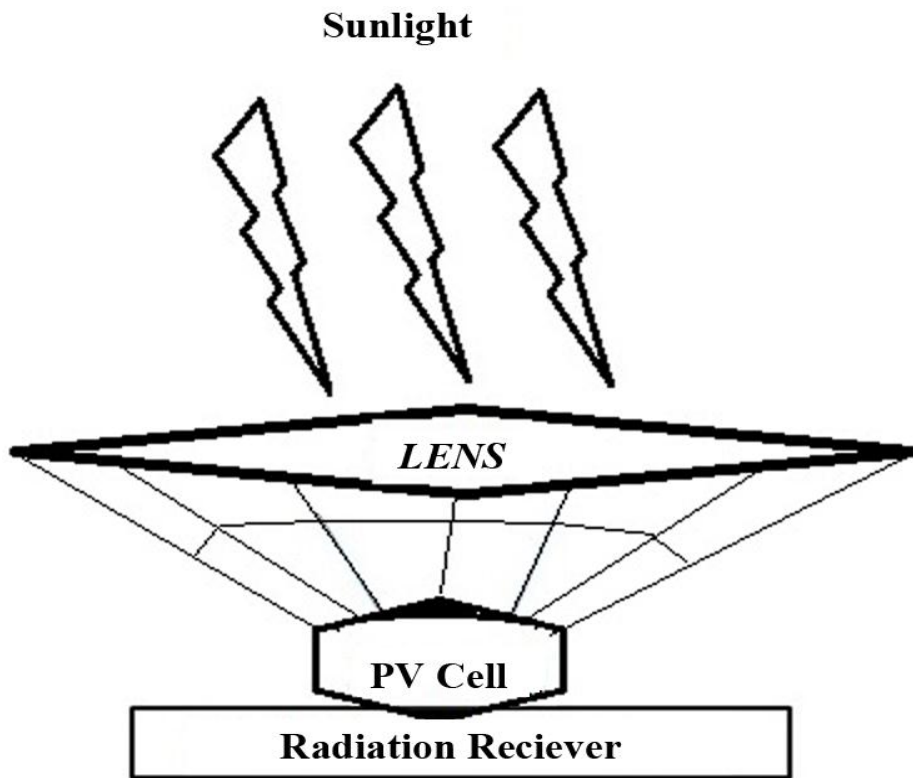


Figure2.1 Schematic of concentrated solar cells [38].

2.7 Various types of solar cell technologies and current trends of development

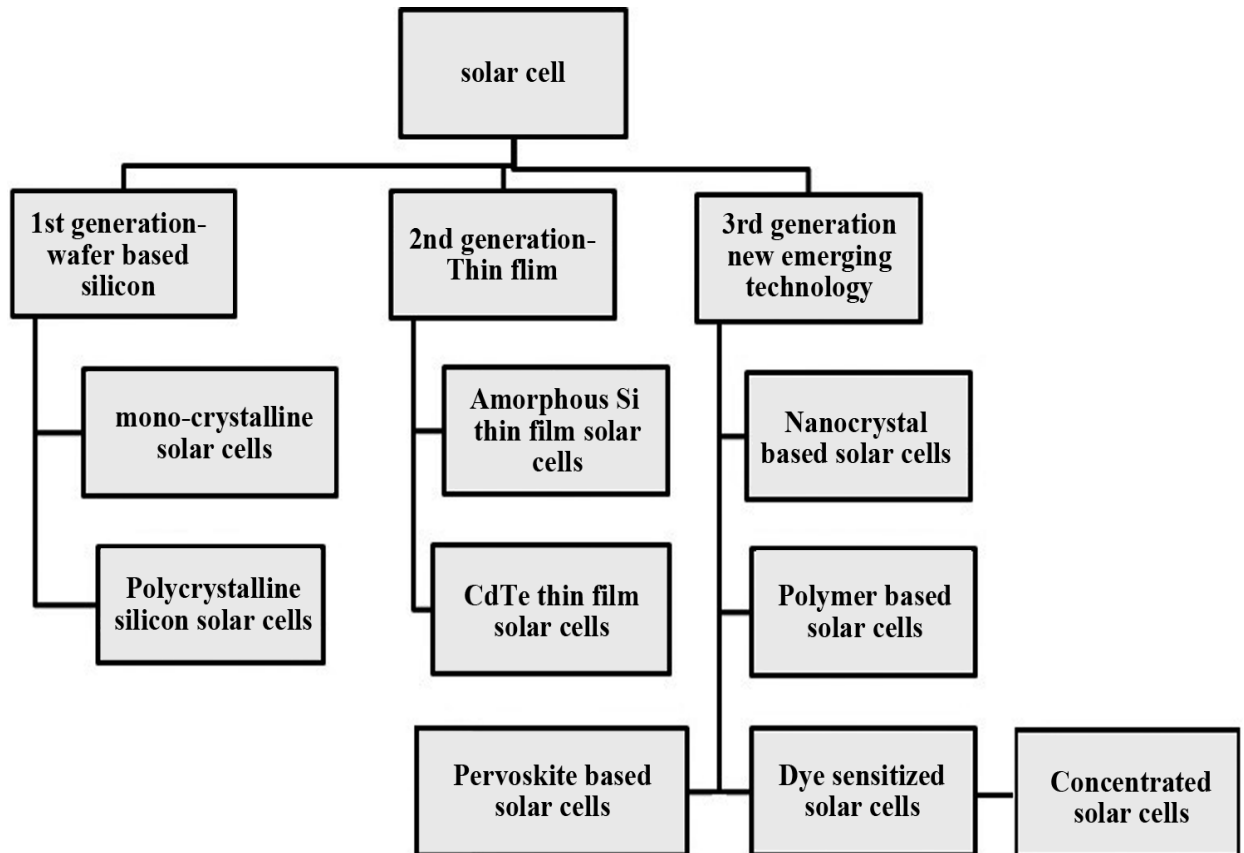


Figure 2.2 Various types of solar cell technologies and current trends of development [38].

2.8 The Potential of Photovoltaic

Photovoltaic is able to convert sunlight directly into electricity and so allows to create an independent power supply. Solar cells can generate power in remote areas, because they do not rely on energy sources other than sunlight. In principle, the average sunshine over an area only as large as Wales (UK) would already be sufficient to supply the world's electricity needs. Photovoltaics thus has a great potential to address the world's energy requirement in the long run,

in contrast to conventional resources, which are either finite or which generate pollutants. However, in order to compete with conventional energy technologies, solar cells still need to prove higher power conversion efficiencies and lower costs.

If I first consider what limits the conversion efficiency of sunlight into electricity, optical losses are identified as one of the main loss mechanisms, which will be the focus of this thesis. Thermal loss mechanisms, such as Joule heating, are another key factor affecting the power conversion efficiency. The need for good electrical transport properties does not tolerate material impurities or fabrication importations, hence electrical loss mechanisms are also important, especially as the cost pressure in the solar industry makes it often too expensive for industry to use high purity materials [39].

A new development in photovoltaic therefore needs to move below the trend curve of silicon wafers; in order to be competitive and to justify investments. One way to achieve this is to reduce the material thickness, thereby reducing material cost, while maintaining cell efficiency. Their cells rely on light, trapping i.e. on increasing the absorption length by efficiently scattering the light inside the cell [40].

2.9 Dye Sensitized Solar Cells (DSSC)

Recent research has been focused on improving solar efficiency by molecular manipulation, use of nanotechnology for harvesting light energy [41,42]. The first DSSC solar cell was introduced by Michel Gratzel in Swiss federal institute of technology [43,44]. DSSCs based solar cells generally employ dye molecules between the different electrodes. The DSSC device consists of four components: semiconductor electrode (n-type TiO_2 and p-type NiO), a dye sensitizer, redox mediator, and a counter electrode (carbon or Pt) [45]. The DSSCs attractive due

to the simple conventional processing methods like printing techniques, are highly flexible, transparent and low cost as well [46]. The novelty in the DSSC solar cells arise due to the photosensitization of nano grained TiO_2 coatings coupled with the visible optically active dyes, thus increasing the efficiencies greater than 10% [47,48,49,50]. However, there are certain challenges like degradation of dye molecules and hence stability issues [51]. This is due to poor optical absorption of sensitizers which results in poor conversion efficiency. The dye molecules generally degrade after exposure to ultraviolet and infrared radiations leading to a decrease in the lifetime and stability of the cells. Moreover, coating with a barrier layer may also increase the manufacturing more expensive and lower the efficiency [52].

2.10 THE advanced fluorescent concentrator concept

Photonic concepts are used in increase the efficiency of a photovoltaic system is the fluorescent concentrator. A main difference to the examples discussed until now is that in this concept, our instruments are not applied to a solar cell directly, but to a concentrating device to which the solar cell is attached [53]. The task, however, is the same: keep the relevant photons in the device so that they are used by the solar cell. Our instruments in this research are photonic structures that show spectral selectivity. Fluorescent or luminescent concentrators are a concept well-known since the late 1970s (Weber 1976, Goetzberger 1977) [54]. Unlike other concentrating systems, these devices are able to concentrate both direct and diffuse radiation tracking. In a fluorescent concentrator, dye molecules in a dielectric matrix absorb radiation and emit light with a longer wavelength in random directions. Total internal reflection traps most of the emitted light and guides it to solar cells, which are optically coupled to the edges or the bottom of the concentrator. In a stack of fluorescent concentrators, each concentrator with a different dye collects a different part of

the solar spectrum. These different parts can be used by solar cells which are especially efficient in the spectral region of the emission of the dye in the concentrator or which they are attached. The solar cells can be interconnected with a high degree of freedom [55].

Research in those days aimed at reducing costs by using the concentrator to reduce the need for expensive solar cells. However, several problems occurred that led to reduced research interest. First, the used organic dyes had only relatively narrow absorption bands. Secondly, although available dyes showed a good performance in the visible spectrum, no suitable dyes were found for the infrared. Reabsorption of the emitted light due to overlapping absorption and emission spectra further reduced efficiencies (Wittwer 1981).

Another main problem was the escape cone of total internal reflection, which caused losses of at least 26%. The value of 26% is obtained for a refractive index of $n=1.5$ and the assumption of isotropic emission. Based on conceptual progress and new materials, several groups are currently reinvestigating the potential of fluorescent concentrators [56].

2.11 Substrates

DSC construction typically makes use of printing technology for the deposition of device layers. The fabrication processes are thus low cost and easy to implement. Which allow the deposition of the needed amount of material only, also reducing the impact on the environment. Furthermore, these methods are compatible with batch (mainly glass substrates) and roll-to-roll production methods (metal and plastic foils). Transparent conducting electrodes are typically realized by deposition of transparent conducting oxides (ZnO). Among the various choices, F:SnO (FTO) offers better performance for glass substrates, because this type of material can withstand the high temperatures layer without degradation of its conductivity [57].

2.12 FTO glass

FTO (Fluorine-doped tin oxide) glass is transparent conductive metal

oxide that can be used in the fabrication of transparent electrodes for thin film photovoltaic, such as: organic photovoltaic, amorphous silicon, cadmium telluride, dye sensitized solar cells, and [58] FTO glass also has a varied range of other applications, including touch screen displays, electromagnetic interference/radio frequency interference shielding, heated glass, anti-static coatings, and light-emitting diodes. There are several properties of FTO glass that make it suitable for the fabrication of a wide range of optoelectronic devices: these include low surface resistivity, high optical transmittance, scratch and abrasion resistant, thermally stable up to high temperatures, and inert to a wide range of chemicals[59].

2.12.1 Fluorine doped Tin Oxide (FTO) glass

Fluorine doped tin oxide (FTO) exhibits good visible transparency owing to its wide band-gap, while retaining a low electrical resistivity due to the high carrier concentration (N_d) caused by the oxygen vacancies and the substitutional fluorine dopant [60]. FTO is mechanically, chemically and electrochemically stable [61], and it is utilized in numerous technologies including; thin film solar cells [62], dielectric layers in low emissivity coatings for windows [63], in gas sensors applications [64] and in liquid crystal displays [65]. There are a number of methods/techniques to grow ZnO (either doped or un-doped) films, including chemical vapor deposition [66], pulsed laser deposition [67], DC reactive sputtering [68] and spray pyrolysis [69]. Some techniques require a high substrate temperature to deposit the film, which can often cause the formation of intermediate semiconductor oxide layers at the film boundary [70]. Any post-treatment of the films, such

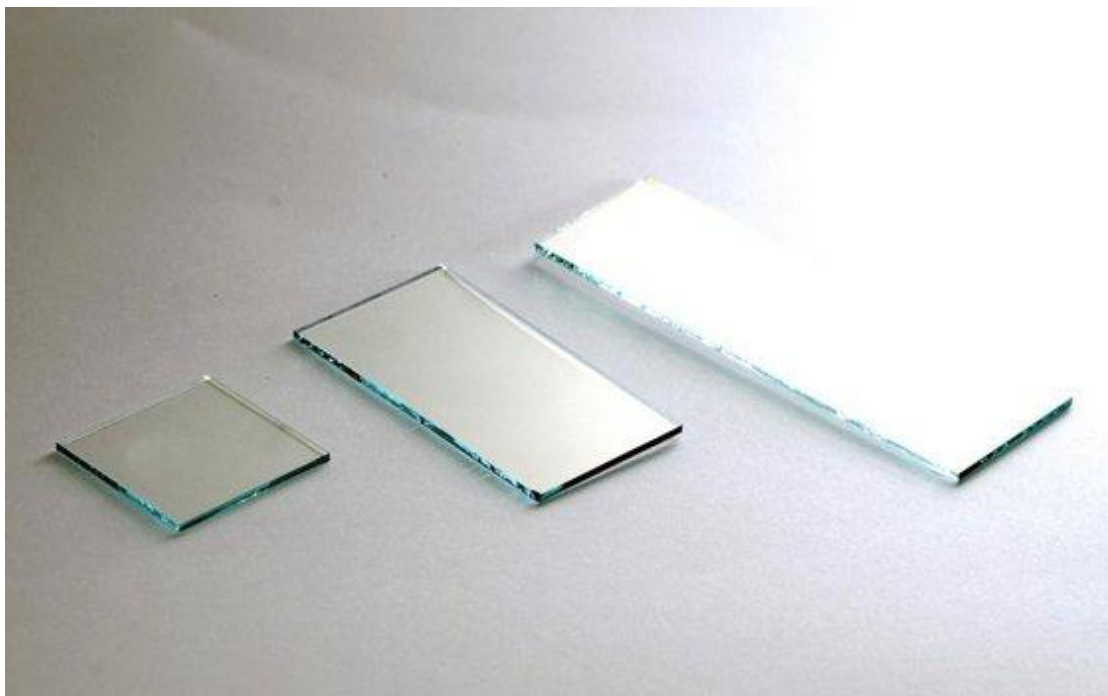
as annealing, also poses additional operational costs and reduced throughput. A few attempts have been made to sputter FTO from solid targets using techniques such as RF magnetron sputtering [71].

2.12.2 Features and benefits of FTO

Electrically conductive for heated and thermal control, electrostatic dissipation and reduced transmittance of electromagnetic radiation.

Color neutral glass inhibits reflector color, increases light transmittance and minimizes haze to optimize clear visibility.

Easily fabricated durable pyrolytic surface can be handled, cut, insulated, laminated, heat-strengthened and tempered using standard techniques [72].



Figur 2.3 FTO glass

2.13 ZnO nanostructures

Nanostructures of ZnO can be synthesized into a variety of morphologies including nanowires, Nanorods, tetrapods, Nanobelts, Nanoflowers, nanoparticles etc. Nanostructures can be obtained with most above-mentioned techniques [73,74] . nanostructures of ZnO can be produced via aqueous methods, which are attractive for the following reasons: They are low cost, less hazardous citation needed, and thus capable of easy scaling up; the growth occurs at a relatively low temperature, compatible with flexible organic substrates; there is no need for the use of metal catalysts, and thus it can be integrated with well-developed silicon technologies. In addition, there are a variety of parameters that can be tuned to effectively control the morphology and properties of the final product. Wet chemical methods have been demonstrated as a very powerful and versatile technique for growing one-dimensional ZnO nanostructures [75,76]. Doping of the ZnO nanowires has been achieved by adding other metal nitrates to the growth solution [77].The morphology of the resulting nanostructures can be tuned by changing the parameters relating to the precursor composition (such as the zinc concentration and pH) or to the thermal treatment (such as the temperature and heating rate)[78]. Presiding substrates with ZnO creates sites for homogeneous nucleation of ZnO crystal during the synthesis. Common pre-seeding methods include in-situ thermal decomposition of zinc acetate crystallites, spin coating of ZnO nanoparticles and the use of physical vapor deposition methods to deposit ZnO thin films[79,80] .Presiding can be performed in conjunction with top down patterning methods such as electron beam lithography and nanosphere lithography to designate nucleation sites prior to growth. Aligned ZnO nanowires can be used in dye sensitized solar cell and field emission devices [81,82].

2.13.1 Electrical properties

ZnO has a relatively large direct band gap of ~ 3.3 eV at room temperature. Advantages associated with a large band gap include higher breakdown voltages, ability to sustain large electric fields, lower electronic noise, and high-temperature and high-power operation. The band gap of ZnO can further be tuned to $\sim 3\text{--}4$ eV by its alloying with magnesium or cadmium oxide [83]. Most ZnO has n-type character, even in the absence of intentional doping. nonstoichiometric is typically the origin of n-type character, but the subject remains controversial [84] . Electron mobility of ZnO strongly varies with temperature and has a maximum of ~ 2000 $\text{cm}^2/(\text{V}\cdot\text{s})$ at 80 K [85]. Data on hole mobility are scarce with values in the range $5\text{--}30$ $\text{cm}^2/(\text{V}\cdot\text{s})$ [86].

2.14 Facile synthesis of ZnO nanoparticle on FTO glass for dye-sensitized solar cells

ZnO nanostructures .As one of the typical 1D ZnO nanoparticle, ZnO nanowires have great potential in electronic and optoelectronic device applications, such as piezo-nanogenerators, electroluminescent devices, field-emission devices , and solar cells. At present, ZnO nanoparticle can be synthesized through various techniques, including physical vapor deposition chemical vapor deposition laser ablation, and the solution method. Because the solution method has the merit of low temperature, large scale, and economical synthesis, it has attracted the interest of numerous researchers worldwide. As with the previous solution methods, which derive from a seed layer, it usually requires the preparation of a layer of uniform and high-quality ZnO film. There are two main ways to prepare such a ZnO seed layer: sputtering and wet coating. The former requires expensive equipment and complex conditions .The latter usually requires several cycles of wet coating and annealing which restricts the reliability and reproducibility of the fabrication process of ZnO nanoparticles. In this work, we

presented a simplified approach to pre-prepare a ZnO seed layer on FTO substrate through one-time spin-coating followed by annealing. Long and well-aligned ZnO nanoparticle synthesized based on this ZnO seed layer. The effect of refreshing the growth solution on the morphology of ZnO nanowires had been investigated and the possible mechanism was also discussed. The application of ZnO nanostructure with various growth cycles into dye-sensitized solar cells showed that the prepared ZnO nanoparticle possessed excellent photovoltaic performance [87].

2.15 Dyes

The purpose of the dye is to absorb as much light as possible and inject the photo-excited electrons into the conduction band of the semiconductor. It must function in a wide thermal range and maintain photo stability for long-term use [88].

2.15.1 Types of dyes

There are many dye types:

2.15.1.1 Inorganic dye

Includes metal complex, such as poly pyridyl (complex of ruthenium and osmium) [89].

2.15.1.3 Natural dyes

Dyes derived from natural materials are exclusively used for educational purpose representing a low-cost and environmentally friendly alternative to conventional Ru-complex. Extracted dyes might also be a good starting point to evaluate, which dyes classes are potentially interesting for sensitization, example of natural dyes blackberries gave a conversion efficiency of 0.056% [91].

2.16 Organic complex of other metals:

Other metal complex have been securitized for their application in DSSC, among them Os- ,Pt ,and Fe-complex .however the overall conversion efficiency is only 50% of standard Ru-dye .Pt-complex give modes efficiencies of 0.7% and iron-complex ,which are very interesting due to the vast abundance of the metal and its non-toxicity are at a very low efficiency level at the moment 0.3%[92].

2.17 Rose Bengal

Rose Bengal (4,5,6,7-tetrachloro-2',4',5',7'-tetraiodofluorescein) is a stain . Its sodium salt is commonly used in eye drops to stain damaged conjunctiva and conceal cells and thereby identify damage to the eye The stain is also used in the preparation of foraminifera for microscopic analysis, allowing the distinction between forms that were alive or dead at the time of collection. A form of rose Bengal is also being studied as a treatment for certain cancers and skin conditions. The cancer formulation of the drug, known as PV-10, is currently undergoing clinical trials for melanoma and breast cancer The Company also has formulated a drug based on rose Bengal for the treatment of eczema and psoriasis, this drug, PV-10, is currently in clinical trials as well.

2.17.1 History and etymology

Rose Bengal was originally prepared in 1882 by Ghnem, as an analogue of fluorescein its name derives from rose (flower) and Bengal (region); it is printed as rose Bengal or Rose Bengal in the scientific literature. [93]

2.17.2 Chemical applications

Despite its complicated photochemistry involving several species, rose Bengal is also used in synthetic chemistry to generate singlet oxygen from triplet oxygen. The singlet oxygen can then undergo a variety of useful reactions, particularly [2+ 2] cycloadditions with alkenes and similar systems [94].

2.18 Nile blue

Nile blue (or Nile blue A) is a stain used in biology and histology. It may be used with live or fixed cells, and imparts a blue color to cell nuclei. It may also be used in conjunction with fluorescence microscopy to stain for the presence of polyhydroxybutyrate granules in prokaryotic or eukaryotic cells. Boiling a solution of Nile blue with sulfuric acid produces Nile red (Nile blue oxazone).

2.18.1 Chemical and physical properties

Nile blue is a fluorescent dye. The fluorescence shows especially in non-polar solvents with a high quantum yield. The absorption and emission maxima of Nile blue are strongly dependent on pH and the solvents used [95].

2.19 Solvent

Table 2.1 Absorption λ_{\max} (nm) and Emission λ_{\max} (nm) for solvent

Solvent	Absorption λ_{\max}(nm)	Emission λ_{\max} (nm)
Acetone	499	596
Chloroform	624	647
Ethanol	628	667
Methanol	626	668
Benzene	635	674

2.19.1 Physical Properties of Solvents

Table 2.2 Physical Properties of Solvents

Solvent name	Density	Viscosity cp20 °C	Melting Point(°C)
Methanol	0.791	0.55	-98
Ethanol	0.816	1.10	-144
Acetone	0.791	0.32	-9
Chloroform	1.492	0.58	-64
Benzene	0.874	0.65	6

2.20 Oxides

Many review articles about oxides have been published but most of them concentrate on specific properties such as electrical conductivity [96], simultaneously high optical transparency and electrical conductivity [97], photoconductivity [98], dielectric constant [99], catalysis [100], electronic structure [101], among others. The wide range of properties of oxides, not only suggests, but demonstrates the versatility of oxides as functional materials. Indeed, the potential of these important materials can be exploited to enhance the performance of opto-electronic devices such as photovoltaic (PV) cells. It follows that an assessment of the various oxides available and how their properties can be used in PV cells would be useful for the researcher looking to enhance the photo-conversion efficiencies above the present day levels while keeping the device cost as low as possible. In general, different materials are required to perform different functions in a PV cell, namely:

- The absorber is responsible for absorption and conversion of incident photons to charge carriers;

- Electrodes are necessary to convey the photo-generated carriers to an external load;
- Antireflection coatings (ARCs) are applied to PV cells to ensure a gradual increase of the refractive index as incident photons traverse from air through to the absorber so as to reduce the backward reflection losses;
- Back reflectors are used to prevent energy waste when the absorber is too thin to absorb all the incident photons in one pass;
- Buffers and/or barriers are used to prevent irregularities at interfaces from affecting PV cell performance. These may be defect states caused by lattice mismatch, too large energy band offsets or diffusion of contaminants into the absorber, among others.

2.21 Oxides of Precious Metals

The precious metals consist of Cu, Ag and Au all of which exhibit the highest room temperature electrical conductivity and reflectivity of known metals. Due to cost restrictions, it is doubtful that oxides containing significant amounts of Au and Ag would be used in solar cells. In the quest to find low cost materials, there is a revival in the research of copper oxide based PV cells since copper can form different oxides and thus the band gap can be tuned from 1.4 eV for CuO to 2.1 eV for Cu₂O [102]. It is however, reported in the literature that the p-type cuprous oxide Cu₂O with a band gap of ~2 eV can be used as a photovoltaic absorber [103,104].

2.22 Oxides of Fusible Metals

The fusible metals group consists of zinc, cadmium, mercury, gallium, indium, thallium, tin, lead, antimony and bismuth, all of which have relatively low melting points. The highest melting point is 419 °C for zinc and 630.63 °C for antimony [105]. The oxides of zinc (ZnO), cadmium (CdO), gallium (Ga₂O₃), indium (In₂O₃) and tin SnO₂ possess a wide optical band gap, a large energy

separation between the CBM and the second conduction band ensuring high visible light transparency; a low CBM with respect to the vacuum level, for high durability, as well as a small effective mass, for high electron mobility. The metal cations of these TCOs have an electronic configuration of the form $(n-1)d^{10}ns^0$ and thus the spherical nature of the vacant s orbitals form highly dispersed conduction bands with small effective electron masses allowing high electron mobility's [106]. These so-called s-type metal oxides form a class of materials known as transparent conductive oxides which find widespread use in PV cells. On the other hand, in SnO, PbO, Sb₂O₃ and Bi₂O₃, the s orbital is fully occupied and therefore lies inside the valence band, the electrons are donated from the p-orbital [107] and thus these oxides are nominally p-type. Presently, the search for a p-type transparent semiconductor with conductivity and transparency similar to the known n-type TCOs is a subject of intense research [108,109].

At normal pressure and temperature, ZnO crystallizes in the wurtzite form with layers occupied by zinc atoms alternating with layers occupied by oxygen atoms. The Zn atoms are tetrahedral coordinated to four atoms, where the Zn 3d-electrons hybridize with the O 2p-electrons. The conduction band minimum is dominated by Zn 4s states while the top of the valence band maximum is mainly made up of O 2p states. Intrinsic ZnO is an n-type conductor and depending on the deposition and treatment procedure, n-type doping may be achieved via Zn interstitials or oxygen vacancies although, many groups have observed unintentional doping caused by residual hydrogen which is a low level donor [110]. The substitution of Zn on lattice sites by Al [111].

2.23 Oxides in Contemporary Photovoltaic Cell Technologies

One of the earliest reports of improved PCE attributed to the presence of an oxide was for a so-called antireflection coated metal oxide semiconductor PV

cell consisting of a GaAs |Au schottky barrier. Although, the device made use of a Ta₂O₅ antireflection coating, the determining factor was the oxidation of the GaAs surface before coating with the gold which lead to an increase in open circuit V_{OC} and a remarkable relative efficiency jump of ~7%, in absolute terms, to 15% under terrestrial sunlight. Since then oxide coatings feature in different types of PV cells for the purpose of light management (reflectors, anti-reflection coatings and light scatters), photo-carrier generation, charge carrier transport, defect passivation, band alignment and charge carrier blocking, among others. Several photovoltaic cell technologies based on materials such as silicon wafer, CdTe, CuInGa(S,Se) and thin film silicon have reached maturity and are available on the market to the general public. Other types of PV cells, especially those with the promise of low material cost, such as organic based, are the subject of intense research efforts. Yet further back the chain, new materials are being synthesized and device configurations suitable to achieve high efficiencies still have to be designed. In this section, a brief description of the operation of contemporary PV cells is given and the role of oxides in such devices discussed [112].

2.24 Ideal Material Characteristics for Various Functions in PV Cells

In order to identify those oxides that are suitable for use in PV cells, it is important to familiarize oneself with the ideal material requirements for high power conversion efficiency (PCE). All PV cells consist basically of a semiconductor material capable of absorbing a certain portion of the solar spectrum and adjacent layers (electrodes) required to extract the photo-generated carriers for conveyance to an external electrical load. Therefore, the optical and electronic properties of each material in the PV cell should be tuned to prevent unnecessary loss of incident photons through reflection and parasitic absorption, as well as, to minimize loss of the photo-generated power via recombination at

trap states and electrical resistance losses. Additionally, the PV cells should maintain their initial efficiency over a lifetime of at least 20 years and should therefore not only be mechanically stable, but also resistant to degradation caused by exposure to the environment [113].

2.25 High Efficiency Concepts

To overcome the SQ limit, the following general approaches can be employed:

1. Adjustment of electron levels to the energy of incoming photons, for example impurity solar cells and intermediate band solar cells
 2. Optimization of photo carrier kinetics, such as photo carrier multiplication (impact ionization), multi-exciton generation, and other ways to use energy of hot electrons. Adjustment of photons to the electron levels in the photovoltaic material, for example photon up-conversion, photon down-conversion, and light management to redirect solar light at the angle corresponding to the disk of the sun
- This section reviews the technical approaches aimed at overcoming the SQ limit with discussion on how these approaches work in current and emerging photovoltaic technologies, such as multijunction PV devices, up- and down-conversion of solar radiation, impurity band solar cell, intermediate band cell, and hot electron conversion. Prior to discussing recent ideas based on numerous possibilities provided by achievements in nanotechnology, note that the only technology that results in an efficiency that exceeds the SQ limit is multijunction solar cells. This system was designed to target the issue of thermalization losses while converting broadband radiation. It employs a set of junctions, each designed for effective harvesting and conversion of a specific spectral range near the material band gap [114,115]. A two junction cell can reach 42% efficiency, and three-junction cells can achieve 49% efficiency [116]. In devices with five or more junctions the ultimate efficiency may even reach ~70%. However, current technology enables only triple-junction cells. This is mainly due to limitations

and high cost of multijunction devices as determined by the need for lattice match, thermal expansion match, and current match in a cascade of p–n (n–p) junctions [117]. Nonetheless, multijunction cells demonstrate record high power conversion efficiencies (~42%) under concentration [118].

2.26 Efficiency limitations

A traditional solid-state p-n device has an upper theoretical limit of 33% power conversion efficiency from light to electricity. The thermodynamic limit for this process in general is 93%, and it is believed that this can be approached by stacking thin films of different properties on top of each other or by inventing fundamentally new concepts [119].

2.27 Background on Hybrid Photovoltaic

Organic/inorganic hybrid solar cells are attracting growing attention and becoming a vibrant field of research. All inorganic solar cells have higher efficiencies due to their excellent carrier mobility, but are generally expensive. The low-cost polymer solar cells, on the other hand, often lacks air stability and satisfactory performance due to inferior transport properties. Combining these two types of materials offers a potential solution to create the next-generation of low-cost, efficient solar cells. Numerous hybrid devices have been demonstrated. However, common processing techniques for polymers, including spin-coating, inkjet printing, or doctor blading (only applicable to planar substrates) result in noncom formal coatings or thickness gradients when applied to three-dimensional morphology, and interface engineering. The total thickness for the light-harvesting active layer in solution-processed photovoltaic is only a few hundred nanometers. This allows for low cost and flexible architectures, with processes compatible with roll-to-roll manufacturing for high-volume production. To date, one of the main challenges is to unravel the complex

selection of degradation phenomena that occurs in this type of optoelectronic device. Photolytic and photochemical reactions are activated under illumination directly from the polymer, degrading the conversion efficiency over time in ambient atmosphere [120]. In order to provide the highest efficiency at reasonable prices, hybrid photovoltaic technologies emerge to combine the benefits of organic and inorganic materials. The photovoltaic layer is typically constituted of semiconducting polymers intimately mixed with inorganic Nanocrystals or other nanostructures. The classical inorganic solar cells mentioned earlier have higher carrier mobility; whereas organic solar cells benefit from considerably higher optical absorption coefficients. The charge transfer in this new class of photo junctions can be studied in composites of p-type conjugated polymers with n-type inorganic semiconductors, or vice versa [121].

2.28 Characterizing performance of solar cells

Regardless of the type of solar cell, they can be compared in terms of how well they perform. Four different parameters are typically listed:

Open circuit voltage, short circuit current, fill factor and efficiency.

A fifth definition, maximum power point, is also used in some of the parameters. Open circuit voltage refers to the potential difference between the two electrodes when there is no external circuit to allow for current. *Short circuit current* is the current flowing between the two electrodes when they are connected externally without any resistance. The maximum power point (*mp*) is where the voltage V and the current density J of a solar cell are such that their product P_{max} is maximized. [122].

$$P_{max} = V_{mp} \times J_m \dots \dots \dots (2.1)$$

Fill factor is defined as the maximum achievable power divided by the theoretical power at short circuit current and open-circuit voltage [123].

As the quality of the solar cell goes up, this value approaches.

$$FF = P_{max} \div I_{sc} \times V_{oc} \dots\dots\dots (2.2)$$

The power conversion efficiency η of a solar cell is the ratio between output electric power density and input light power density. P_{max} and E are usually given in mW/cm^2 for laboratory purposes [124].

$$\eta = P_{max} \div E \dots\dots\dots (2.3)$$

Chapter Three

Literature Review

3.1 Introduction

Different attempts were made to fabricate solar cells to increase efficiency and decrease cost. Here we caught some of them study the factors that affect performance of solar cells.

3.2 A study on the reliability and performance of solar powered street lighting systems

This work presents the results of a study on the reliability and performance of the solar-powered street lighting systems installed at the African University of Science and Technology (AUST) in Nigeria, a hot and humid environment. The technical performance of the systems was studied using the following performance indicators: system energy yield, capture loss, as well as the system performance ratio while the reliability of the systems was examined using a model developed from the findings from the maintenance and fault diagnosis of the systems. The model was used to predict the total failure and survival probability of the systems using the Weibull distribution. The performance evaluation during the monitored period (February 2012 to January 2015) indicated that the performance ratios of the systems vary from 70% to 89% and the energy yields of the systems ranging from 2.87 h/day to 5.57 h/day. The results from the reliability analysis also showed that when the stress concentration factor around the notch between the cable terminals in the charge controller increases, the charge controller will become overheated, which in turn affected other components of the systems. The implications of this study are also

discussed for the design and development of future solar-powered street lighting systems in some of them polymers were used to fabricate cheap cells.

3.5 High Voltage All Polymer Solar Cells with a Polymer Acceptor based on NDI and Benzotriazole

Qing Maa,d, Xiaonan Xueb, Lian Zhonga,d, Indunil Angunawelac, Shanshan Chene,Harald Ade,c*Lijun Huo,b*Zhanjun Zhang,a*and Yongfang Lia,d* (This journal is © The Royal Society of Chemistry 2019)

All –polymer solar cells (all-PSCs) with a p-type conjugated polymer as a donor and an n-type conjugated polymer an acceptor have attracted increasing attention recently due to their good film-forming properties, excellent flexibility and high morphological stability. Herein, we synthesized a new n-type conjugated copolymer LA03 based on naphthalene dioxide (NDI)and benzotriazole (BTZ)with thiophene π -bridges, which is a structure modification of N2200 by inserting a benzotriazole units. Compared with N2200, LA03 exhibits blue –shifted absorption and higher lowest unoccupied molecular orbital (LUMO) energy level. The LA03-based all-PSCs with wide band gap polymer PBDB-T as a donor, achieved a power conversion efficiency (PCE) of 6.49%, with a high open circuit voltage (V_{oc}) of 0.937V, which is improved in comparison with the PBDB –T: N2200-based all-PSCs with a PCE of 5.85% and a V_{oc} of 0.812 V. the higher V_{oc} of the LA03-based devices is benefitted from the up –shifted LUMO energy level of the LA03 acceptor. The results indicate that inserting benzotriazole unit into the main chain of N2200is an effective way to upshift its LUMO energy level and increase the V_{oc} of the all-PSCs.

3.6 Comprehensive Study on Chemical and Hot Press-Treated Silver Nanowires for Efficient Polymer Solar Cell Application

Yang-Yen Yu 1,2,* , Yo-Jen Ting 1, Chung-Lin Chung 1, Tzung-Wei Tsai 1 and Chih-Ping Chen 1,* (Received: 13 October 2017; 17 November 2017; Published: 22 November 2017)

In this study, chemical treatment (CT; oxidation–reduction method) and physical treatment (HP; hot-pressing methods) were applied to improve the performance of silver nanowire (AgNW)-derived electrodes on a glass or flexible polyethylene terephthalate (PET) substrate.

The four-point probe method, UV-Vis spectroscopy and scanning electron microscopy (SEM) were used to measure the properties of AgNW electrodes and compare them with those of indium tin oxide (ITO) electrodes for exploring the possibility of using CT- and HP-based AgNW electrodes for polymer solar cell (PSC) applications. Using the CT or HP method, the sheet resistance of electrodes decreased to lower than 40 Ω/sq with an average high transmittance of more than 80%. Furthermore, HP reduced the surface roughness of AgNWs, which solved the inter-electrode short circuiting problem for devices. We studied the performance of poly(3,4-ethylenedioxythiophene)-poly(styrene sulfonate) and zinc oxide-based PSC devices. The power conversion efficiency of HP-AgNW-derived poly[4,8-bis(5-(2-ethylhexyl)thiophen-2-yl)benzo[1,2b;4,5-b₀]dithiophene-2,6-diyl-alt-(4-(2-ethylhexyl)-3-fluorothiophen-3,4-b₀)thiophene-2-carboxylate-2,6-diyl] (PTB7-Th):[6,6]-phenyl-C71-butyric acid methyl ester (PC71BM) devices was 7.83%, which was slightly lower than the performance of the device using ITO (8.03%) as a substrate. After a bend test (100 times) at a 2-cm curvature radius, the efficiency of AgNW/PET-derived PSCs was more than 70%. The performance of PSCs made with AgNWs and ITO electrodes is comparable, but the cost of using AgNWs for electrodes is much lower;

therefore,HP-derived AgNWs demonstrate great potential for optoelectronic applications. Used Zinc Oxide to obtain high stability

3.7 Synthesis and characterization of zinc oxide nanoparticles: application to textiles as UV-absorbers

Alessio Becheri, Maximilian Dürer, Pierandrea Lo Nostro, Piero Baglioni
Received: 16 July 2007 / Accepted: 30 September 2007 / Published online: 30 October 2007

In this report the synthesis and characterization of nanosized zinc oxide particles and their application on cotton and wool fabrics for UV shielding. The nanoparticles were produced in different conditions of temperature (90 or 150°C) and reacting medium (water or 1,2-ethanediol). A high temperature was necessary to obtain small monodispersed particles. Fourier transformed infrared spectroscopy (FTIR), transmission electron microscopy (TEM), and X-ray powder diffractometry (XRD) were used to characterize the nanoparticles composition, their shape, size and crystallinity. The specific surface area of the dry powders was also determined. ZnO nanoparticles were then applied to cotton and wool samples to impart sunscreen activity to the treated textiles. The effectiveness of the treatment was assessed through UV–Vis spectrophotometry and the calculation of the ultraviolet protection factor (UPF). Physical tests (tensile strength and elongation) were performed on the fabrics before and after the treatment with ZnO

Nano particles.

3.8 Fully Printed Zinc Oxide Electrolyte-Gated Transistors on Paper

José Tiago Carvalho 1 , Viorel Dubceac 1 , Paul Grey 1, Inês Cunha 1, Elvira Fortunato 1, Rodrigo Martins 1, Andre Clausner 2, Ehrenfried Zschech 2 and Luís Pereira 1,* (Received: 28 December 2018; Accepted: 22 January 2019; Published: 30 January 2019)

Fully printed and flexible inorganic electrolyte gated transistors (EGTs) on paper with a channel layer based on an interconnected zinc oxide (ZnO) nanoparticle matrix are reported in this work. The required rheological properties and good layer formation after printing are obtained using an eco-friendly binder such as ethyl cellulose (EC) to disperse the ZnO nanoparticles. Fully printed devices on glass substrates using a composite solid polymer electrolyte as gate dielectric exhibit saturation mobility above $5\text{cm}^2\text{V}^{-1}\text{s}^{-1}$ after annealing at 350°C . Proper optimization of the nanoparticle content in the ink allows for the formation of a ZnO channel layer at a maximum annealing temperature of 150°C , compatible with paper substrates. These devices show low operation voltages, with a sub threshold slope of 0.21V dec^{-1} , a turn on voltage of 1.90V , a saturation mobility of $0.07\text{cm}^2\text{V}^{-1}\text{s}^{-1}$ and an Ion/Ioff ratio of more than three orders of magnitude.

3.9 Functional behaviour of paper coated with zinc oxide – soluble starch Nano composites

Prasad, V., Shaikh, A.J., Kathe, A.A., Bisoyi, D.K., Verma, A.K., Vigneshwaran, N., Functional behaviour of paper coated with zinc oxide -soluble starch nanocomposites, *Journal of Materials Processing Technology* (2010)

Zinc oxide (ZnO) is a potential pigment material for paper coating to impart brightness and better printing properties. Nano-ZnO, due to its extremely small size, gives paper coating pigment a high covering power apart from antifungal

and UV protecting properties. In this work, zinc oxide soluble starch Nano composites (nano-ZnO) was prepared by a simple and novel wet chemical method using zinc nitrate and sodium hydroxide as precursors and soluble starch as stabilizing agent. Primary

Particle size distribution was extracted from small angle X-ray scattering (SAXS) measurements by the hard sphere model and calculated to have an average size of 4.1nm. This nano-ZnO was coated on the surface of base paper (59 GSM) in a laboratory paper coater and their properties were studied. The brightness, whiteness, paper smoothness, print density, print uniformity, picking velocity and oil absorbency of nano-ZnO coated paper showed significant improvement than that of bulk ZnO coated paper. In addition, the nano-ZnO coated paper showed excellent anti-fungal and UV protecting properties that are much essential to enhance the life of a paper.

In the other attempts amorphous poly crystalline and Nano silicon solar cells were also fabricated to increase efficiency.

3.10 Nano-Photonic Structures for Light Trapping in Ultra-Thin Crystalline Silicon Solar Cells

Prathap Pathi ^{1,2}, Akshit Peer ³ and Rana Biswas ^{4,*}(Published: 13 January 2017)

Thick wafer-silicon is the dominant solar cell technology. It is of great interest to develop ultra-thin solar cells that can reduce materials usage, but still achieve acceptable performance and high solar absorption. Accordingly, we developed a highly absorbing ultra-thin crystalline Si based solar cell architecture using periodically patterned front and rear dielectric Nano cone arrays which provide enhanced light trapping. The rear Nano cones are embedded in a silver back reflector.

In contrast to previous approaches, we utilize dielectric photonic crystals with a completely flat silicon absorber layer, providing expected high electronic quality and low carrier recombination.

This architecture creates a dense mesh of wave-guided modes at near-infrared wavelengths in the absorber layer, generating enhanced absorption. For thin silicon (<2 μm) and 750 nm pitch arrays, scattering matrix simulations predict enhancements exceeding 90%. Absorption approaches the Lambert and limit at small thicknesses (<10 μm) and is slightly lower (by ~5%) at wafer-scale thicknesses. Parasitic losses are ~25% for ultra-thin (2 μm) silicon and just 1%–2% for thicker (>100 μm) cells. There is potential for 20 μm thick cells to provide 30 mA/cm² photo-current and >20% efficiency. This architecture has great promise for ultra-thin silicon solar panels with reduced material utilization and enhanced light-trapping.

3.11 High Efficiency Silicon Solar Cells

Andrew Blakers^a, Ngwe Zina, Keith R. McIntosh^b, Kean Fong^a (PV Asia Pacific Conference 2012)

Silicon remains the material of choice for photovoltaic because of its abundance, non-toxicity, high and stable cell efficiencies, the maturity of production infrastructure and the deep and widespread level of skill available in relation to silicon devices. Rapidly decreasing module prices mean that area-related balance of systems costs are an increasing proportion of photovoltaic systems price. This places a premium on efficient cells. In recent years there have been large improvements in mass production of high quality wafers, the ability to handle thin wafers, maintenance of high minority carrier lifetimes, surface passivation, and minimization of optical losses, device characterization and in other areas. Many of these improvements are viable in mass production. The upper limit of

silicon solar cell efficiency is 29%, which is substantially higher than the best laboratory (25%) and large-area commercial (24%) cells.

Cell efficiencies above 25% appear to be feasible in both a laboratory and commercial environment. Such a cell will have minimal bulk recombination due to a combination of a thin substrate with a very high minority carrier lifetime; superb surface passivation; small-area electrical contacts consistent with low contact recombination, free carrier absorption and contact resistance; excellent optical control through the use of texturing, antireflection coatings and rear surface reflectors; low edge recombination assisted by the use of thinner wafers, larger cells and edge passivation; and sufficient metal coverage to minimize resistive losses. This paper will survey current work in high performance silicon solar cell design and fabrication, and discuss approaches to efficiency improvements.

3.12 Fabrication and Characterization of Rose Bengal Sensitized Binary TiO₂-ZrO₂ Oxides Photo-electrode Based Dye-sensitized Solar Cells

(M. A. Waghmare , N. I. Beedri , A. U. Ubale and H. M. Pathan January 2019)

Titanium oxide (TiO₂) electrode has been the most commonly used photo-electrode for the dye-sensitized solar cells (DSSCs). Several research groups have already reported that only TiO₂ layer is not yet ideal for electron transfer in the absence of space charge layer and also demonstrated the procedures for coating nanocrystalline semiconducting oxide films with a thin overcoat of a different semiconducting oxide with a higher conduction band energy level (E_c). Zirconium oxide (ZrO₂) is a suitable material for such overcoat because of its higher E_c. The binary TiO₂ -ZrO₂ oxide photo-electrodes were prepared by doctor blading technique. The electrodes were annealed at 450C and then sensitized by Rose Bengal (RB) dye. The DSSC fabricated by binary TiO₂ -ZrO₂

photo-electrode showed improved solar energy conversion efficiency than that of fabricated only by pure component of TiO_2 .

3.13 Preparation of Fluorine-doped Tin Oxide by a Spray Pyrolysis Deposition and Its Application to the Fabrication of Dye-sensitized Solar Cell Module

(S. Kaneko, S. Kawasaki, P. V. V. Jayaweera and G. R. A. Kumara June 13-17, 2010)

Spray pyrolysis technique is the most suitable process to deposit uniform large area thin film, where a thin film is deposited by spraying a starting solution on heated surface and then constituents react to form a new solid phase. This technique is particularly useful for the deposition of oxides and has long been production method for applying a transparent conducting tin oxide to glass substrate. Fluorine doped tin oxide (FTO_2) has been recognized as a very promising material for a number of optoelectronic applications, because it is quite stable for atmospheric conditions, chemically inert, mechanically hard, high-temperature resistant, etc. Spray pyrolysis deposition (SPD) technique has been employed to prepare large area fluorine-doped tin oxide (FTO), Nano crystalline TiO_2 and catalytic Pt films for dye-sensitized solar cell (DSC) module. The transparent conducting FTO film gave low sheet resistance $8 \Omega/\text{cm}$ and average visible light transmittance exceeded 80 %. Large area ($15 \times 15 \text{ cm}^2$) DSC module prepared here shows efficiency 7.4 % at AM-1.5 simulated sun light.

3.14 Solar cells based on synthesized nanocrystalline ZnO thin films sensitized by chlorophyll a and photopigments isolated from spinach(Kristian Nygren(03- 2010)

The work done by Kristian Nygren studies. Synthesized nanocrystalline ZnO thin films sensitized by chlorophyll a as well as isolated photopigments from spinach leaves. The nanocrystals were studied using XRD, and it was confirmed that three different methods of synthesis resulted in ZnO crystals of a few nanometers. The solar cells were assembled with Au electrodes in a sandwich configuration and their photovoltaic properties were investigated. Overall light to electricity conversion was low with the highest efficiency being 0.21%. An astonishingly low efficiency of 0.0003% was noted for a thin film which was not thermally treated, and it is suggested that heat-treatment is of great importance. It was also found that photopigments from spinach can be extracted easily and used as molecular sensitizer without any demanding purification steps.

3.15 Facile synthesis of ZnO nanowires on FTO glass for dye-sensitized solar cells

34(7):074002 · July 2013 (Carminna _and_ Ottone)In the work done by Carminna and Ottone: Long and well-aligned ZnO nanowires were hydrothermally synthesized on FTO glass based on a ZnO seed layer which was prepared by spin-coating and annealing techniques. The effect of the growth solution refreshment on the morphology of ZnO nanowires was investigated and the possible mechanism was discussed. After refreshing the growth solution for 5 cycles, ZnO nanowires of ~ 120 nm in diameter and ~ 20 μm in length were obtained. The prepared ZnO nanowires were used as photo electrodes in dye-sensitized solar cells (DSSCs), showing excellent photovoltaic performance. With the increase of growth cycles of ZnO nanowires, the photocurrent of DSSCs increased obviously due to the increased dye loading on the surface of ZnO nanowires. The results indicated

that the long and well-aligned ZnO nanowires are promising for DSSCs application. The simplified method of preparing ZnO seed layer on FTO substrate is favorable to improve the reliability and reproducibility of the fabrication process of ZnO nanowires. After growing for 5 cycles, ZnO nanowires of 20m in length have been obtained. Dye-sensitized solar cells (DSSCs) with the prepared ZnO nanowires as photo electrodes exhibited excellent photovoltaic performance. With the increase of growth cycles of ZnO nanowires, the photocurrent of DSSCs increases obviously. The conversion efficiency of DSSC with ZnO nanowire of 5 growth cycles was improved by more than 2 times compared with that of only 1 growth cycle due to the increased dye loading on the surface of ZnO nanowires. The present results imply that the long and well-aligned ZnO nanowires are promising materials for DSSCs and other optoelectronic applications.

3.16 Comparison of transparent conductive indium tin oxide, titanium-doped indium oxide, and fluorine-doped tin oxide films for dye-sensitized solar cell application

(Dong-Joo Kwak and Byung-Ho Moon 2011) Dong-Joo Kwak and Byung-Ho Moon et al investigated.

In this study, we investigate the photovoltaic performance of transparent conductive indium tin oxide (ITO), titanium-doped indium oxide (ITiO), and fluorine-doped tin oxide (FTO) films. ITO and ITiO films are prepared by radio frequency magnetron sputtering on soda-lime glass Substrate at 300 °C, and the FTO film used is a commercial product. One measure the X-ray diffraction patterns, AFM micrographs, transmittance, and sheet resistances after heat treatment, and transparent conductive characteristics of each film. The value of electrical resistivity and optical transmittance of the ITiO films is $4.15 \times 10^{-4} \Omega\text{-cm}$. The near-infrared ray transmittance of ITiO is the highest for wavelengths

over 1,000 nm, which can increase dye sensitization compared to ITO and FTO. The Photo conversion efficiency (η) of the dye-sensitized solar cell (DSC) sample using ITiO was 5.64%, whereas it was 2.73% and 6.47% for DSC samples with ITO and FTO, respectively, both at 100mW/cm² light intensity.

3.17 Using Gum Arabic in Making Solar Cells by Thin Films Instead Of Polymers

Abdalsakhi and Mubarak Dirar Abd-alla (Jan. - Feb. 2016) 8, Issue 1 Ver. III, PP 27-32

In the paper Abdalsakhi, gum Arabic based solar cells with Rhodamine 6G were fabricated on indium tin oxide by a spin coater position. Microstructure and cell performance of the solar cells with ITO/ Rhodamine 6G/ Gum Arabic structures were investigated. Photovoltaic devices based on the Rhodamine 6G / Gum Arabic heterojunction structures provided photovoltaic properties under illumination. Absorption and energy gap measurement of the Rhodamine 6G / Gum Arabic heterojunction were studied by using UV-VIS mini 1240 spectrophotometer and light current-voltage characteristics. The three ITO/Gum/Rhodamine/Au solar cells were produced and characterized, which provided efficiency (η) having values (3.8 - 5.1 and 5.2) %. Fill factor (FF) is (0.964 - 0.9462 and 0.973), current density (J_{sc}) is (2.22 - 4.31 and 4.4) mAcm⁻² and Open – circuit voltage (V_{oc}) is (1.22 -1.25 and 1.209) V. The application of conducting Arabic Gum to optoelectronic devices such as solar cell, light emitting diodes, and electrochemical sensors are of practical significance, because the Arabic Gum mixture can be easily prepared and modified by rich chemical products to meet optical and electronic requirements. This solar cell is cheap can be easily fabricated. Its efficiency is relatively large.

3.18 Applications of Oxide Coatings in Photovoltaic Devices

Helmholtz and Zentrum Berlin für Materialien und Energies GmbH, 10 March 2014 / Published: 244 Due to the diverse applications of oxides in PV cells, new oxide materials are being introduced for use in PV. While the transparent conducting oxides of indium, zinc and tin are important as electrodes in most PV cell technologies, TiO_2 has become the model material for PV cells based on charge transfer to a sensitized semiconductor. The oxides of silicon and aluminum, both members of the semi-metal group, when highly insulating can be used for passivation due to their high dielectric constant. The transition metal oxides with high work functions are now routinely used for organic PV cells as electrode buffer materials to maximise the cell voltage and to prevent leakage currents. Other oxides, such as those of copper and lead have been used as absorber materials. More exotic multinary oxides such as the ferroelectric perovskites BiFeO_3 and KNbO_3 are used as absorbers with the promise of high cell voltage. Lanthanide host oxides and lanthanide doped oxides have been introduced as wide band spectral converters to enhance the spectral response of PV cells beyond the normal absorption band of the absorber material. Much as this review has focused on examples of applications of oxide materials where PV cell performance has been experimentally demonstrated, the contribution and importance of theoretical calculations towards these and future developments cannot be overstated. Upland Metalloid and metal based oxides are an almost unavoidable component in the majority of solar cell technologies used at the time of writing this review. Numerous studies have shown increases of $\geq 1\%$ absolute in solar cell efficiency by simply substituting a given layer in the material stack with an oxide. Depending on the stoichiometry and whether other elements are present, oxides can be used for the purpose of light management, passivation of electrical defects, photo-carrier generation, charge separation, and charge transport in a solar cell. In this review, the most commonly used oxides whose

benefits for solar cells have been proven both in a laboratory and industrial environment are discussed. Additionally, developing trends in the use of oxides, as well as newer oxide materials, and deposition technologies for solar cells are reported.

3.19 Electro deposition of In_2S_3 Thin Films onto FTO Substrate from DMSO Solution

B. Marí1, M. Mollar1 and D. Soro2, 46022,(1 March 2013)

B. Marí1, M. Mollar1 and others study the electrochemical deposition of In_2S_3 thin films from a $\text{In}(\text{ClO}_4)_3$ and S8 in dimethyl sulfa oxide (DMSO) solution. SEM micrographs exhibited complete substrate coverage whereas EDAX analysis gave In/S ratio very close to 2/3. Grazing XRD analysis showed that the films were grown in the tetragonal phase without the presence of oxide or hydroxide phases as usually is reported in aqueous medium. Results open the possibility of applying the procedure to the electro deposition of an alternative In_2S_3 buffer layer onto copper indium diselenide substrates for evaluating the performance of the corresponding solar cell.

3.20 Polymeric Materials for Conversion of Electromagnetic Waves from the Sun to Electric Power

(2018 by, Licensee MDPI,Basel.) In work of Licensee, etal they investigate the photovoltaic performance of transparent conductive indium tin oxide (ITO), titanium-doped indium oxide (ITiO), and fluorine-doped tin oxide (FTO) films. ITO and ITiO films are prepared by radio frequency magnetron sputtering on soda-lime glass substrate at 300 °C, and the FTO film used is a commercial product. They used XRD technique beside AFM micrographs and transmittance, sheet resistances after heat treatment, and transparent conductive characteristics of each film. The value of electrical resistivity and optical transmittance of the

ITiO films is $4.15 \times 10^{-4} \Omega\text{-cm}$. The near-infrared ray transmittance of ITiO is the highest for wavelengths over 1,000 nm, which can increase dye sensitization compared to ITO and FTO. The photo conversion efficiency (η) of the dye-sensitized solar cell (DSC) sample using ITiO was 5.64%, whereas it is 2.73% and 6.47% for DSC samples with ITO and FTO, respectively, both at 100mW/cm^2 light intensity. Solar photoelectric energy converted into electricity requires large surface areas with incident light and flexible materials to capture these light emissions. Currently, sunlight rays are converted to electrical energy using silicon polymeric material with efficiency up to 22%. The majority of the energy is lost during conversion due to an energy gap between sunlight photons and polymer energy transformation. This energy conversion also depends on the morphology of present polymeric materials. Therefore, it is very important to construct mechanisms of highest energy occupied molecular orbitals (HOMO)_s and the lowest energy unoccupied molecular orbitals (LUMO)_s to increase the efficiency of conversion. The organic and inorganic solar cells used as dyes can absorb more photons from sunlight and the energy gap will be less for better conversion of energy to electricity than the conventional solar cells.

3.21 Rational Design of Solar Cells for Efficient Solar Energy Conversion

(Edited by Alagarsamy Pandikumar, Karaikudi, Tamil Nadu, 2018 John)

The work done by Alagarsamy,etal explained the use of plasmatic nanoparticle dressed ZnO nanostructures involving various structural designs (nanoparticles, Nano rods, Nano flowers, and nanowires, less common ZnO structures) used in DSSCs. clearly, ZnO Nanorods possess a significant advantage over other ZnO nanostructures when incorporated with plasmatic nanoparticles, as the structure itself promotes a more direct pathway for electron movement. It is also necessary to take into account other parameters, such as the size of the active area of the

photoanode, the amount of plasmatic nanoparticles injected, and the type of sensitizer used, Although some of the work has shown promising results for possible commercialization and applicability, these photoanodes still yield low PCE values when compared to TiO₂-based photoanodes. In order to achieve higher PCE values, other alternative materials are still to be explored, such as the incorporation of plasmatic nanoparticles on a mixture of various ZnO nanostructures (nanopellets, nanosheets, nanotubes, nanofibres). Only a few works on DSSCs based on plasmonic nanoparticles on ZnO nanostructures have been reported. Much work is still needed to be done and investigated, especially with different parameters, in order for it to be on par with recent DSSCs that have reported high performance and good stability.

3.22 Photovoltaic Effect on Molecule Couple Ferromagnetic Films of a Magnetic Tunnel Junction

(Pawan Tyagi, , Kentucky-40506, USA DC-20008, USA- 2015)

The paper of Pawan, etal discussed the observation of photovoltaic effect on the molecule coupled ferromagnetic films of a MTJ. OMCs induced strong exchange coupling appeared to modify the magnetic ordering of ferromagnetic electrodes leading to the occurrence of photovoltaic effect. Similar observations are expected with other systems involving magnetic molecules and MTJ with the exposed top FM electrodes. Calculation of energy conversion efficiency with MEMSD will require both, the charge transport study and magnetic studies, such as magnetic force microscopy to quantify the photoactive region. Further studies are recommended for the elucidation of the precise mechanism of photovoltaic effect with the ferromagnetic films. So the economical solar energy conversion to electricity can be boosted by the discovery of fundamentally new photovoltaic mechanism, and a suitable system to realize it with commonly available materials like iron (Fe) and nickel (Ni). This paper reports the observation of

photovoltaic effect on a molecular spintronics device, composed of magnetic tunnel junction (MTJ) and organometallic molecular clusters (OMCs). A prefabricated MTJ with exposed side edges, after enabling the bridging of OMC channels between its two ferromagnetic films, exhibited following phenomenon (i) dramatic increase in exchange coupling, (ii) 3-6 orders current suppression and (iii) photovoltaic effect. This paper focuses on the photovoltaic effect. Control experiments on isolated ferromagnetic films suggested that OMCs neither affected the magnetic properties nor produced any photovoltaic effect; photovoltaic effect was only observed on the ferromagnetic films serving as magnetic electrodes in a MTJ. Present paper invites further investigation of the similar photovoltaic effect on other combinations of MTJs and promising magnetic molecules, like single molecular magnets, organometallic clusters and porphyrins. This research can lead to mass producible and economical spin photovoltaic devices.

3.23 Fabrication and characterization of vacuum deposited fluorescein thin films

(Pasi Jalakanen^{1,2}, Liisa Antila³, Pasi Myllyperkiö³, Teemu Ihalainen⁴ (2016)

In the work done by Myllyperkiö³, et al simple vacuum evaporation technique for deposition of dyes on various solid surfaces has been developed. Thin films of fluorescein were deposited on glass, fluorine tin oxide (FTO) coated glass with and without atomically layer deposited (ALD) nanocrystalline 20 nm thick anatase TiO₂ coating. Surface topology, absorption and emission spectra of the films depend on their thickness and the material of supporting substrate. On FTO covered glass the absorption spectra are similar to fluorescein solution in ethanol. Absorption spectra on ALD-TiO₂ is red shifted compared to the film deposited on bare FTO. The corresponding emission spectra at $\lambda = 458$ nm excitation show various thickness and substrate dependent features, while the

emission of films deposited on TiO₂ is quenched due to the effective electron transfer to the semiconductor conduction band. Contrary to conventional thin film preparation from a solution, typically resulting in monolayer thick samples, the thermal evaporation enables fabrication of much thicker films in a controlled manner. Thermal evaporation in vacuum of the studied dye – fluorescein - can be performed efficiently at relatively low temperatures 150°C - 160°C (melting point of the dye is 310°C). Non-oxidizing conditions and low temperature preserve fluorescein from degradation. The deposition conditions can be accurately controlled and monitored so that single monolayer accuracy can be achieved with rather simple arrangement. It was found that fluorescein absorption and emission spectra change with the film thickness in a non-trivial manner presumably being related to the thickness dependence of the film morphology. With the increase of the film thickness the emission is quenched due to the increased molecule aggregation. Quenching of fluorescence of fluorescein on TiO₂ substrates is observed in films with thickness ranging from 30nm to 600 nm. For all substrates the absorption converges to the same spectrum as the film thickness increases over few hundred nm. The optimal thickness for observation of the strong narrow-band emission depends on both the surface roughness and the dye thickness.

3.24 Recent trends on nanostructures based solar energy applications: A REVIEW

Crystal Growth Centre, Anna University, Chennai-600 025, India Received: September 15, 2012)

The paper of screech etal, reviews some of the current initiatives and critical issues on the improvement of solar cells based on nanostructures and nanodevices. The growing interest in applying nanoscale materials for solving the problems in solar energy conversion technology can be enhanced by the

introduction of new materials such as quantum dots, multilayer of ultrathin nano crystalline materials and the availability of sufficient quantities of raw materials. The inexpensive purification or synthesis of nanomaterial's, deposition methods for the fabrication of thin film structures and easy process control in order to achieve a large-area production within acceptable performance tolerances and high life time expectancy are still the main challenges for the realization (fabrication) of solar cells. Therefore in attaining the main objectives of photovoltaic, the efficiency of solar cells should be improved without any compromise on the processing cost of these devices. Nanotechnology incorporation into the films shows special promise in enhancing the efficiency of solar energy conservation and also reducing the manufacturing cost. Its efficiency can be improved by increasing the absorption efficiency of the light as well as the overall radiation-to-electricity. This would help to preserve the environment, decrease soldiers carrying loads, provide electricity for rural areas and have a wide array of commercial applications due to its wireless capabilities. The solar energy, a boon to the mankind has to be properly channelized to meet the energy demand in the developing countries and solar cell industry can reach greater heights by the incorporation of third Generation solar cell devices and panels based on nanostructures.

Chapter Four

Material and method

4.1 Introduction

At present, ZnO nanoparticles can be synthesized through various techniques, including physical vapor deposition, chemical vapor deposition, laser ablation, and the solution method. Because the solution method has the merit of low temperature, large scale, and economical synthesis, it has attracted the interest of numerous researchers worldwide. As with the previous solution methods, which derive from a seed layer, it usually requires the preparation of a layer of uniform and high-quality ZnO film. There are two main ways to prepare such a ZnO seed layer: sputtering and wet coating. The former requires expensive equipment and complex conditions. The latter usually requires several cycles of wet coating and annealing which restricts the reliability and reproducibility of the fabrication process of ZnO nanoparticles. In this work, we presented a simplified approach to prepare a ZnO seed layer on FTO substrate through one-time spin coating followed by annealing. Long and well-aligned ZnO nanoparticles were synthesized based on this ZnO seed layer. The effect of refreshing the growth solution on the morphology of ZnO nanowires had been investigated and the possible mechanism was also discussed. The application of ZnO nanowires with various growth cycles into dye-sensitized solar cells showed that the prepared ZnO nanoparticle possessed excellent photovoltaic performance.

In order to prepare a seed solution containing ZnO nanoparticles procedures can be adapted the following:

4.2 Materials and Equipment's

The following materials were used in this work

- Potassium hydroxide supplied by CENTRAL DRUG HOUSE(P). Sodium hydroxide supplied by CENTRAL DRUG HOUSE(P).
- Zinc acetate dehydrate $ZnC_4H_6O_4$ (molecular weight =219.51, Density=1.735 g/cm³, purity=99%).
- Distilled water, de-ionized water supplied by medical laboratories labs - Sudan University of science and technology).
- Magnetic stirrer.
- Beaker and conical flask.
- Thermometer (0-100) °C.
- bottle
- A voltmeter
- AVO meter
- FTO glass
- Co₆₀
- ZnO nanoparticle
- Methanol
- Ethanol
- Acton
- Chloroform
- Benzene
- Iodine
- Nile blue dye
- Bengal Rose dye

4.3 Methodology

4.3.1 ZnO preparation

Zinc acetate dehydrate was mixed in absolute methanol (99%)

Then 0.01 M concentration of zinc acetate (274mg) add in 125ml of methanol and stirred ,heated to 60 °C under continuous stirring.



Figure 4.1 heat the solution to 60°C under continuous stirring

109mg of potassium hydroxide(0.03M) concentration , shacked the solution until it become transparent, added drop-wise from potassium hydroxide solution (to heated zinc acetate) under continuous stirred ,then heated to 60°C for 2hours some drops of solution was taken on substrate leave to dry then the sample clean by Ethanol.

4.3.2 The aqueous chemical growth solution

100ml of de-ionized water was added to zinc acetate (400Mm).then some drops of sodium hydroxide was added to the zinc solution.



Figure 4.2 the solution transparent.

Then the seeded substrate loaded having its face down in the aqueous solution and then load the solution inside an oven heated at temperature 90°C for 3 hours and clean carefully the unloaded substrate in de-ionized water then dried .

The samples ready for characterization.

4.4 Methodology for solar cell



Figure 4.3 FTO glass fixed on the board



Figure 4.4 Deposition of ZnO nanoparticles onto FTO glass

4.4.1 Materials and Methods for Nile Blue

Five samples of Dye Sensitized Solar Cells (DSSC) with Nile Blue were fabricated on FTO glass. A clean glass plate with a thin layer of FTO (Fluorine Tin Oxide) is needed. The FTO acts as the first part of the solar cell, the first electrode. For the purpose of the present study Zinc Oxide cells were made following the generally accepted methods. The fabrication process started by preparing the Zinc Oxide and the dye of Nile Blue coated on FTO glass. (FTO + graphite and Iodine) electrode was used to complete the formation of Dye Sensitized Solar Cells (DSSC). The formed sample were characterized by Ultra violet-visible spectroscopy (UV). The Dye Sensitized Solar Cells (DSSC) was made by depositing ZnO and dye on FTO glass substrate. The FTO glasses were firstly cleaned by ethanol and distilled water. Zinc acetate dehydrate was mixed in pure methanol (99%) Then 0.01 M concentration of zinc acetate (274mg) was add in 125ml of methanol and stirred and heated to 60 °C under continuous stirring one added 109mg of potassium hydroxide having (0.03M) concentration, The solution was shaken until it become transparent. One added drop-wise from potassium hydroxide solution (to heat zinc acetate) under continuous stirred, then heated to 60°C for 2hours. Some drops of solution were taken on substrate and left to be dry. The sample was cleaned by Ethanol, Then 3mg of Nile Blue dye dissolved into 0.5ml of high pure (Methanol, Ethanol Acton, Chloroform, Benzene and Water). was deposited on Zinc Oxide .Being inserted electrical circuit the V-I characteristic was found using electric circuit containing (voltmeter, Ammeter, a light source Lamp and a solar cell) .The V-I reading were taken after exposing the solar cell to light. The UV spectrometer was used to display absorption spectrum. Five samples were prepared (FTO/ ZnO/ Blue Nile dye /FTO+ graphite and Iodine) .by using five different solvent (Methanol , Ethanol, Acton, Chloroform and Benzene).

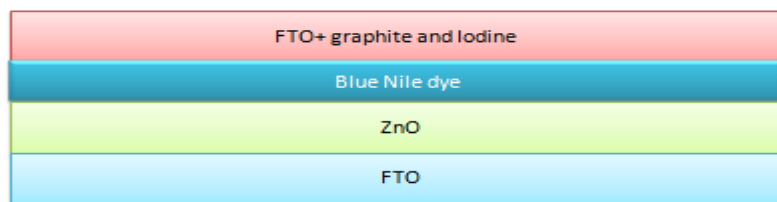


Figure 4.5 schematic structure of (FTO/ ZnO/ Blue Nile dye /FTO+ graphite and Iodine



Figure 4.6 Nile blue dye with (Methanol, Ethanol, Acton, Chloroform and Benzene)

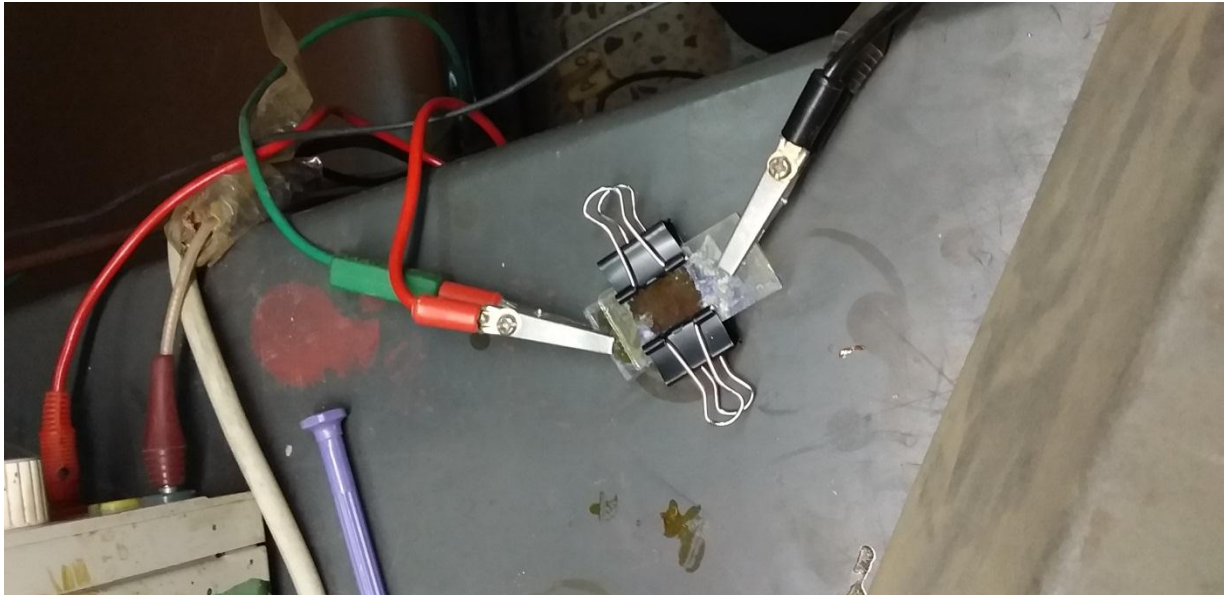


Figure 4.7 Reading (I, V) for solar cell with Nile blue

4.4.2 Materials and Methods for Rose Bengal

Five samples of Dye Sensitized Solar Cells (DSSC) with Rose Bengal were fabricated on FTO glass. A clean glass plate with a thin layer of FTO (Fluorine Tin Oxide) is needed. The FTO acts as the first part of the solar cell, the first electrode. For the purpose of the present study Zinc Oxide cells were made following the generally accepted methods. The fabrication process started by preparing the Zinc Oxide and the dye of Rose Bengal coated on FTO glass. (FTO + graphite and Iodine) electrode was used to complete the formation of Dye Sensitized Solar Cells (DSSC). The formed sample were characterized by Ultra violet-visible spectroscopy (UV). The Dye Sensitized Solar Cells (DSSC) was made by depositing ZnO and dye on FTO glass substrate. The FTO glasses were firstly cleaned by ethanol and distilled water. Zinc acetate dehydrate was mixed in pure methanol (99%) Then 0.01 M concentration of zinc acetate (274mg) was add in 125ml of methanol and stirred and heated to 60 °C under continuous stirring one added 109mg of potassium hydroxide having (0.03M) concentration, the solution was shacked until it become transparent. One added drop-wise from potassium hydroxide solution (to heat zinc acetate) under continuous stirred, then heated to 60°C for 2hours. Some drops of solution were

taken on substrate and left to be dry. The sample was cleaned by Ethanol, Then 3mg of Rose Bengal dye dissolved into 0.5ml of high pure (Methanol, Ethanol Acton, Chloroform, Benzene and Water). was deposited on Zinc Oxide .Being inserted electrical circuit the V-I characteristic was found using electric circuit containing (voltmeter, Ammeter, a light source Lamp and a solar cell) .The V-I reading were taken after exposing the solar cell to light. The UV spectrometer was used to display absorption spectrum. Five samples were prepared (FTO/ ZnO/ Rose Bengal dye /FTO+ graphite and Iodine) .by using five different solvent (Methanol , Ethanol, Acton, Chloroform and Benzene).



Fig 4.8 schematic structure of (FTO/ ZnO/ Rose Bengal /FTO+ graphite and Iodine)



Figure 4.9 Bengal rose dye with (Methanol, Ethanol, Acton, Chloroform and Benzene)



Figure 4.10 Reading (I, V) for solar cell with Bengal rose
The samples ready for characterization

4.5 Results and Discussion for ZnO



Figure 4.11 SEM image of ZnO

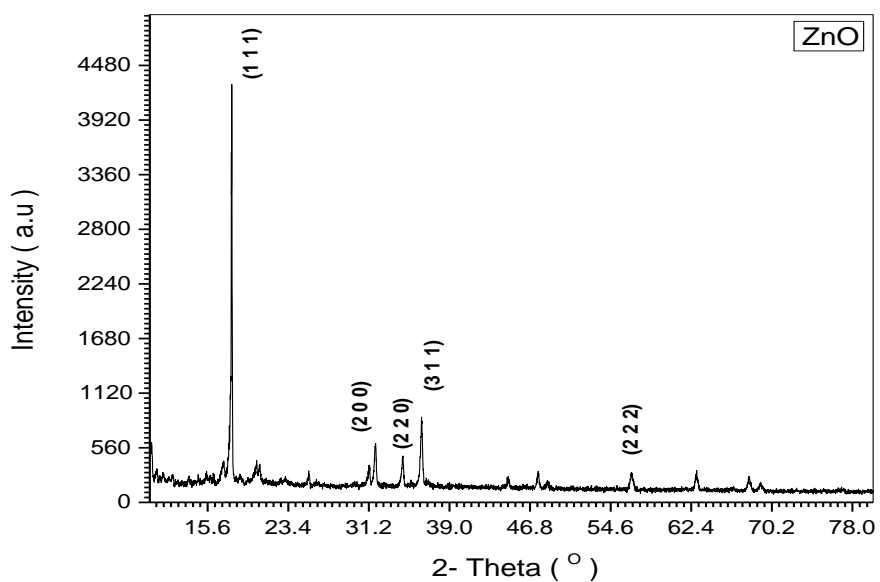


Figure 4.12 XRD spectrum of Nano ZnO sample [Average Lattice Constants = 8.4310/ $a = b = c = 4.629$ / $\alpha = \beta = \gamma = 90^\circ$ / Density = 5.4489 mg.cm⁻³/Crystal Form: Cubic – F- Center Space Group: Fd – 43m (216)

Table 4.1 Lattice Constants from Peak Locations and Miller Indices [Cubic - F-center] of ZnO sample

Solvents	2-Theta	d(A°)	H	K	l	X _s (nm)
Methanol	17.943	2.67255	1	1	1	87.8
Ethanol	31.788	2.31450	2	0	0	47.8
Acetone	34.386	1.63660	2	2	0	53.8
Chloroform	36.438	1.39570	3	1	1	48.8
Benzene	56.594	1.33628	2	2	2	62.3

The crystal structure of ZnO sample was characterized at room temperature using a Philips PW1700 X-ray diffract meter (operated at 40 kV and current of 30 mA) the samples were scanned between 10° and 80° at a scanning speed of 0.06 °C/s using Cu K α radiation with $\lambda = 1.5418\text{\AA}$. The representative XRD charts of ZnO samples as show in fig (4.1). Miller indices provided in the figure and all peaks determine transformation of dried powder to ZnO (111 at 17.943°, 200 at 31.788°, 220 at 34.386°, 311 at 36.438° and 222 at 56.594 °) crystallites with Cubic F-center rutile crystal structure. Table (4.1) shows the XRD parameters of ZnO Nanopowder at various crystalline orientations. The structure of ZnO obtained from the Rietveld refinement is shown in Fig(4.2). Scanning electron micrograph (SEM) of ZnO is shown in Fig(4.2). The SEM is capable of examining large field of view, thus giving sufficient information on the grain growth and its uniformity. The average grain size of ZnO is found to be 63.5nm

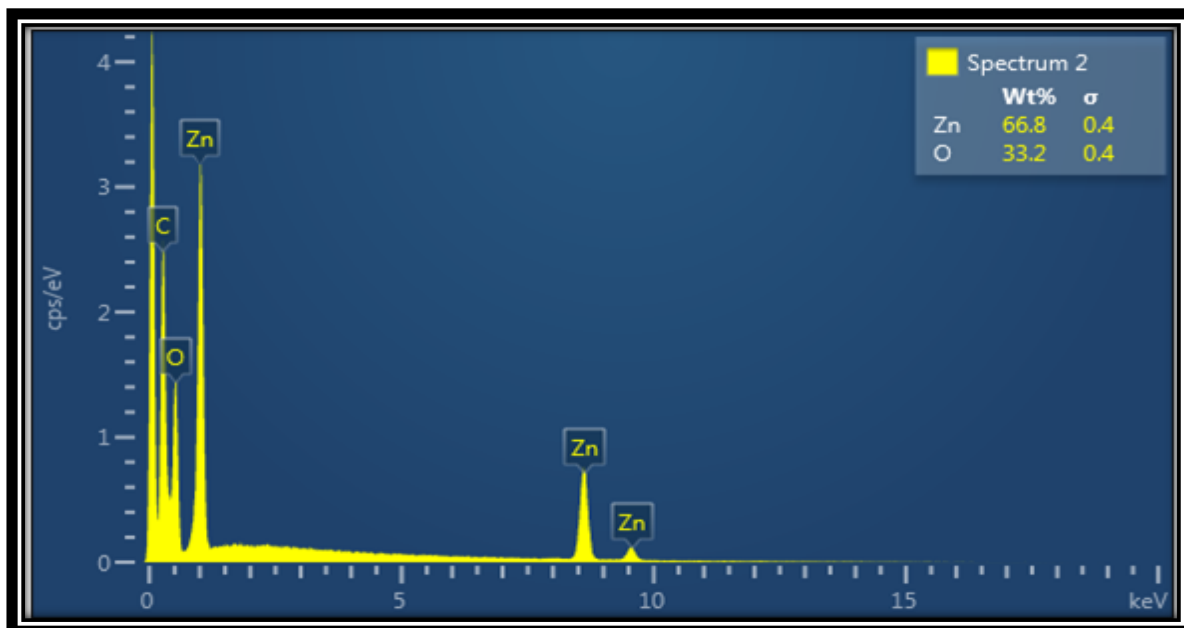


Figure 4.13 EDS spectra of the ZnO Nano sample

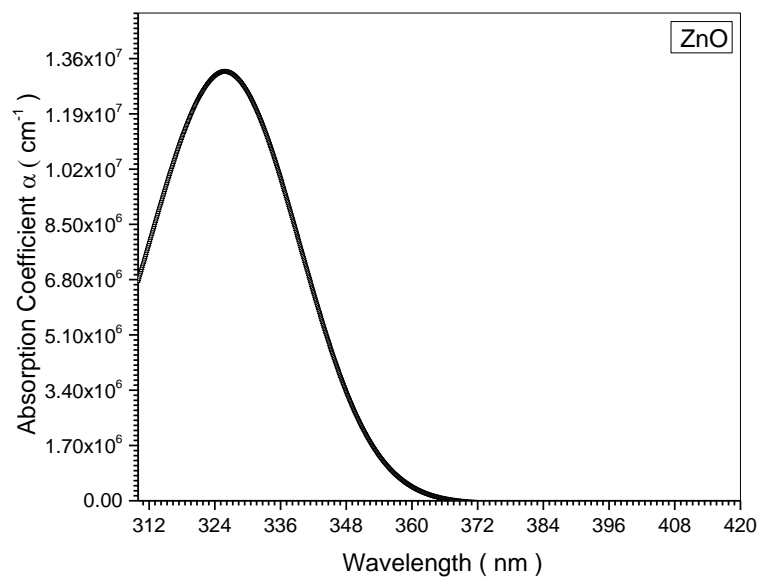


Figure 4.14 relation between Absorption Coefficient (α) and wavelengths of ZnO sample

Fig 4.3 show the EDS spectra of ZnO Nano sample, only two elements, namely, Zn , and O, exist in the sample. The EDS results are shown in fig 4.3. The actual measurements of the metal elements are in good agreement with the nominal composition of the ZnO material. The XRD, SEM, and EDS results show that one obtain a dense and near- stoichiometric ZnO by sintering the sample at fig (4.1) and fig(4.2) , thus showing the suitable sintering condition.

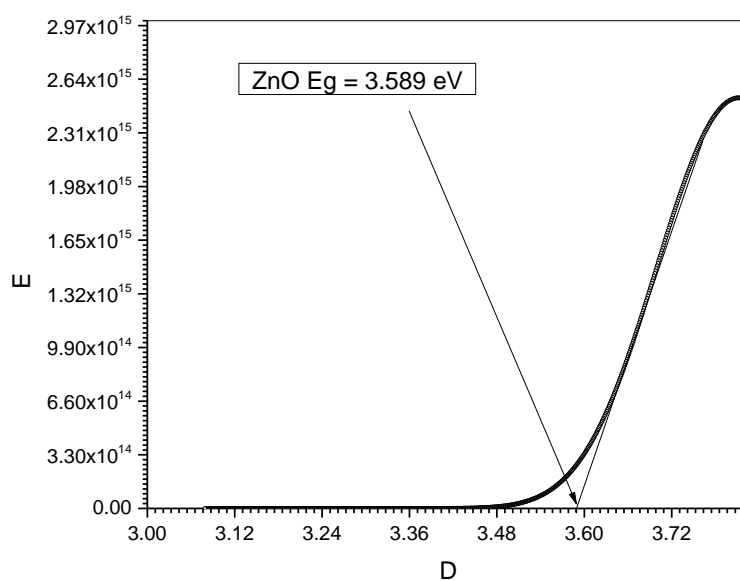


Figure 4.15 Optical Energy Band Gap of ZnO sample

Figure4.16 relation between absorbance and wavelengths of five sample that made by Blue Nile dye in different solvent (Methanol, Ethanol, Acton m Chloroform and Benzene)

4.6 Dye Blue Nile Results and Discussion

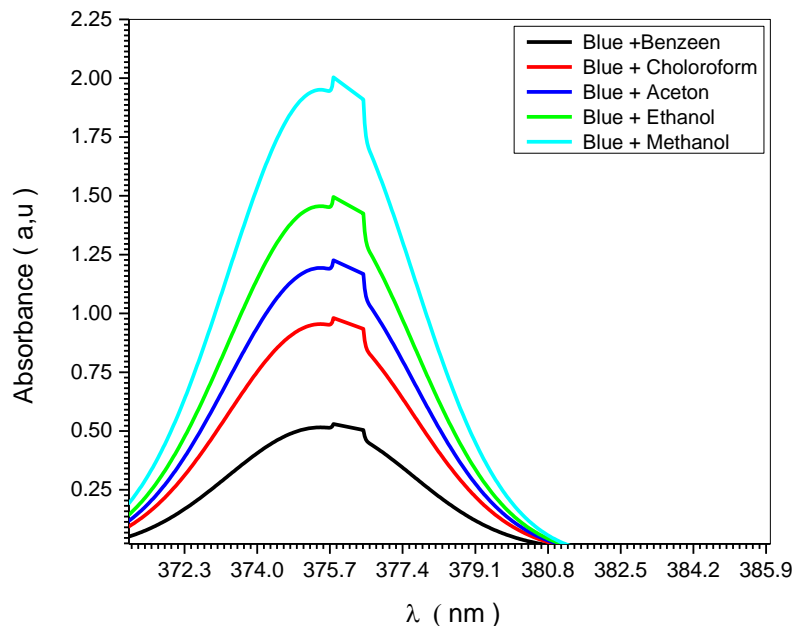


Figure 4.16 relation between absorbance and wavelengths of five samples that were made by Blue Nile dye in different solvents (Methanol, Ethanol, Aceton, Chloroform and Benzene)

In view of figures (4) and (17) it is clear that the addition of the Nile Blue and solvents increases the peak wavelength from about 325 nm to about 375 nm. It also makes the energy gap 3.589 eV more narrow in the range (3.276- 3.296 eV). The efficiency of the solar cells is affected directly by the solvents. The solvent which causes more absorption gives higher efficiency as Fig (25) indicates. This may be due to the fact that more absorption causes more current which increases efficiency. This explanation agrees with the efficiency (η) current density (J) relation in Fig (27).

Fig (26) shows that the efficiency increases as the energy band gap increases. This can be explained by bearing in mind that two factors affect the efficiency, one of them is the density of absorbing atoms that generates more charge carriers

and the energy gap which when increases decreases the number of generated carriers .thus when the effect of increasing atoms density is larger than the effect of increasing the energy gap the efficiency increases.

Table 4.2 Calculate Lattice Constants from Peak Locations and Miller Indices [Cubic Face centered] of ZnO samples

Solvents	2-Theta	d(A°)	H	K	l	X _s (nm)
Methanol	17.943	2.67255	1	1	1	87.8
Ethanol	31.788	2.31450	2	0	0	47.8
Acetone	34.386	1.63660	2	2	0	53.8
Chloroform	36.438	1.39570	3	1	1	48.8
Benzene	56.594	1.33628	2	2	2	62.3

This is since the effect of atom density which generates large carrier's amount is larger than the effect of increasing energy gap which decreases the amount of charge carriers light albeit. The increase of atoms concentration is clear in table (1) for methanol, acetone and Chloroform, where their crystal size are 87.8, 53.8 and 48.8 nm respectively. The large crystal size consists of more atoms than its absorbance is larger as shown in table (2).

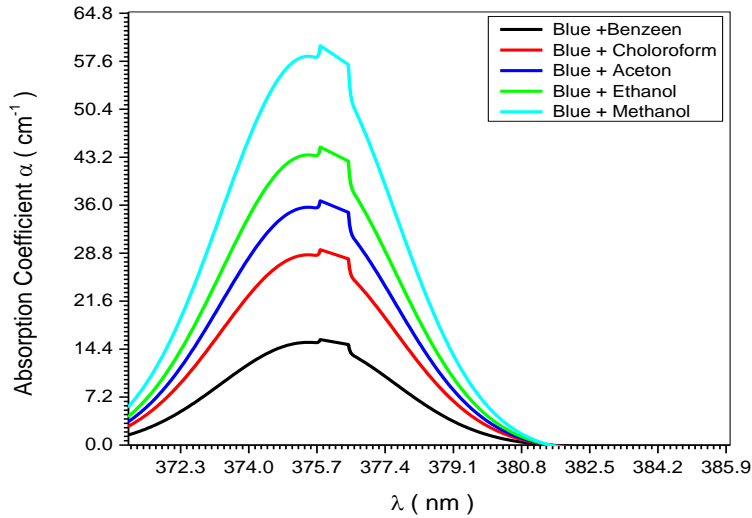


Figure 4.17 relation between absorption coefficient and wavelengths of five sample that made by Blue Nile dye in different solvent, Ethanol, Acton, Chloroform and Benzene) (Methanol, Ethanol = (85.19 cm^{-1}) , Acton = (64.31 cm^{-1}) , Chloroform = (48.12 cm^{-1}) and Benzene = (36.19 cm^{-1})

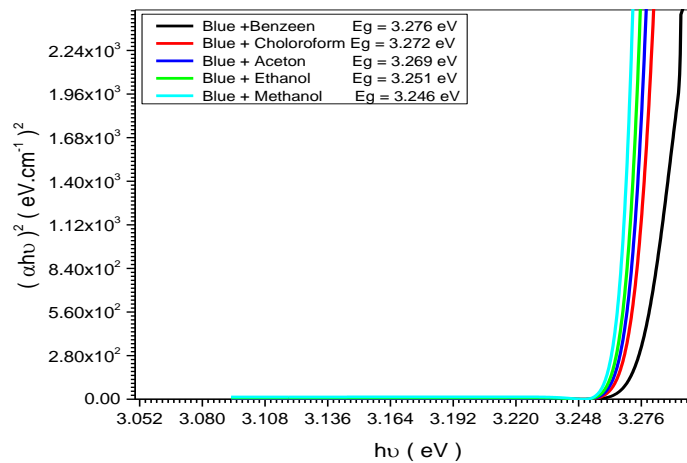


Figure 4.18 the optical energy band gab of five sample that made by Blue Nile dye in different solvent (Methanol, Ethanol, Acton, Chloroform and Benzene)

4.7 Blue Nile Solar Cell Results and Discussion

Table 4.3 Typical I-V riding of Nile Blue with Methanol solar cell

Voltage (mV)	Current (mA)
0	20
2.60709	20.31276
4.84015	20.51557
6.4569	20.51557
7.49956	15.8133
7.6663	8.40686
7.73	0

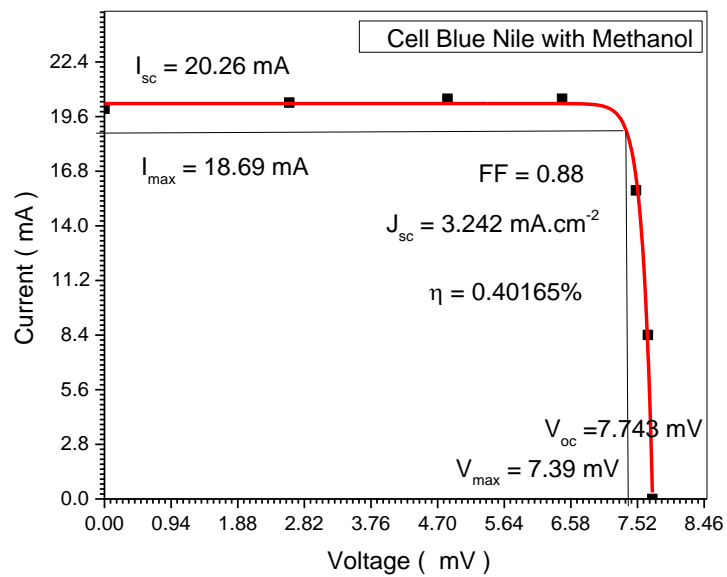


Figure 4.19 several factors for characterization of Nile Blue with Methanol solar cell

Table 4.4 Typical I-V riding of Nile blue with Ethanol solar cell

Voltage (mV)	Current (mA)
0	19.6
2.60709	19.9065
4.84015	20.10526
6.4569	20.10526
7.49956	15.49704
7.6663	8.23872
7.73	0

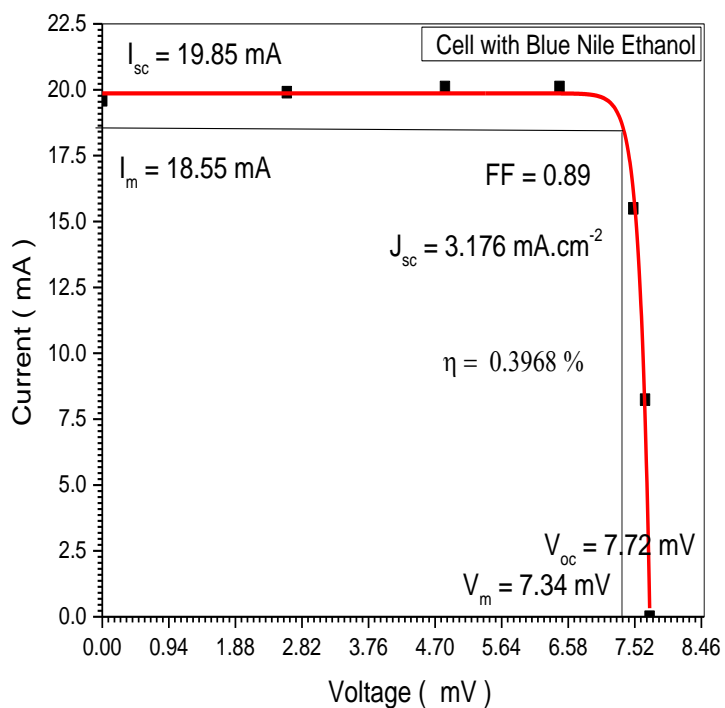


Figure 4.20 several factors for characterization of Nile Blue with Ethanol solar cell

Table 4.5 Typical I-V riding of Nile Blue with Acton solar cell

Voltage (mV)	Current (mA)
0	19.012
2.60709	19.30931
4.84015	19.5021
6.4569	19.5021
7.49956	15.03213
7.6663	7.99156
7.73	0

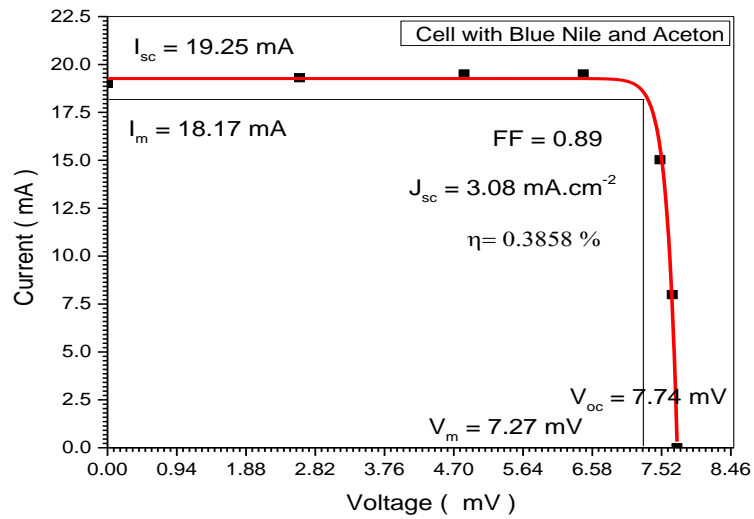


Figure 4.21 several factors for characterization of Nile Blue with Acton solar cell

Table 4.6 Typical I-V riding of Nile Blue with Chloroform solar cell

Voltage (mV)	Current (mA)
0	18.44164
2.60709	18.73003
4.84015	18.91704
6.4569	18.91704
7.49956	14.58116
7.6663	7.75181
7.73	0

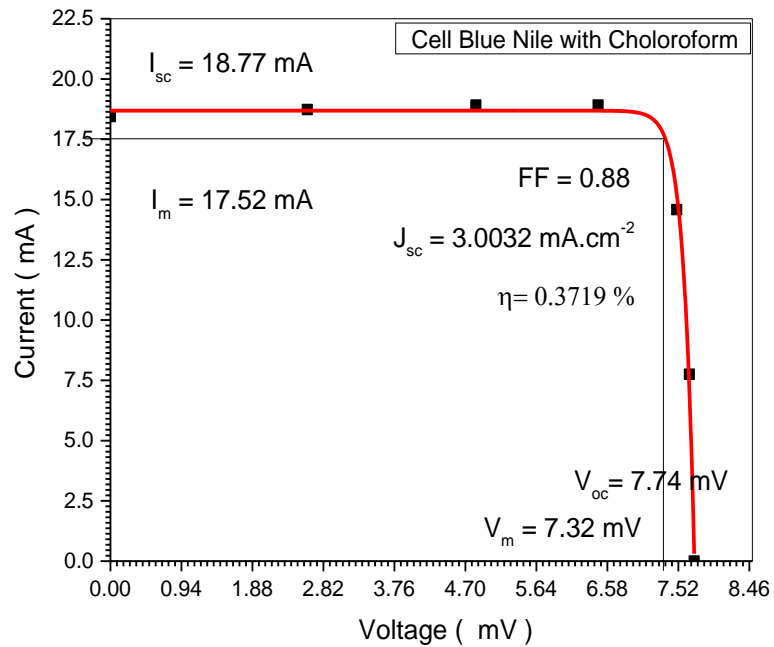


Figure 4.22 several factors for characterization of Nile Blue with Chloroform solar cell.

Table 4.7 Typical I-V riding of Nile Blue with Benzene solar cell

Voltage (mV)	Current (mA)
0	17.33514
2.60709	17.60623
4.84015	17.78202
6.4569	17.78202
7.49956	13.70629
7.6663	7.2867
7.73	0

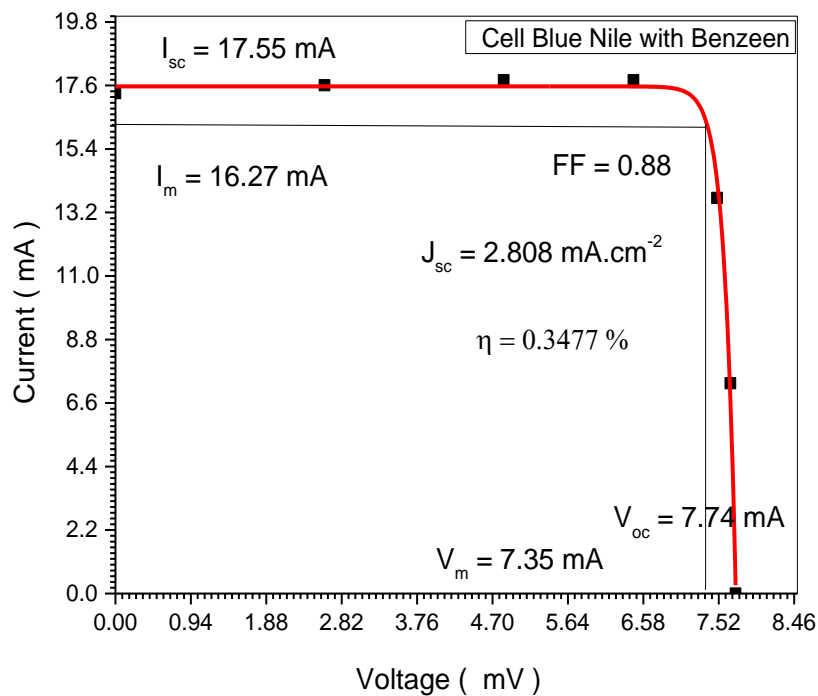


Figure 4.23 several factors for characterization of Nile Blue with Benzene solar cell

Figure (4.15) shows the current-voltage characteristics obtained from the measured values (see Table 4.3) . This measurement was taken from solar cell of the structure (FTO/ ZnO / (Nile Blue with Methanol) dye / Co₆₀ + Iodine

/FTO), The short-circuit current (I_{sc}) is 20.26 mA , the open-circuit voltage (V_{oc}) is 7.743 mV, fill factor (FF) is 0.88, Density of current ($J_{sc}=3.242 \text{ mA.cm}^{-2}$) and the efficiency is ($\eta=0.40165\%$.) Fig (4.16) shows the current-voltage characteristics obtained from the measured values (see Table 4.4) . This measurement was taken from solar cell of the structure (FTO/ ZnO / (Nile Blue with Ethanol) dye / Co₆₀ + Iodine /FTO), The short-circuit current (I_{sc}) is 19.85 mA , the open-circuit voltage (V_{oc}) is 7.72 mV, fill factor (FF) is 0.89, Density of current ($J_{sc} =3.176 \text{ mA.cm}^{-2}$) and the efficiency is ($\eta=0.3968\%$).Fig(4.15) shows the current-voltage characteristics obtained from the measured values (see Table 4.5) . This measurement was taken from solar cell of the structure (FTO/ ZnO / (Nile Blue with Acton) dye / Co₆₀ + Iodine /FTO), The short-circuit current (I_{sc}) is 19.25mA, the open-circuit voltage (V_{oc}) is 7.74mV, fill factor (FF) is 0.89, Density of current ($J_{sc}=3.08 \text{ mA.cm}^{-2}$) and the efficiency is ($\eta=0.3858\%$). Fig (4.16) shows the current-voltage characteristics obtained from the measured values (see Table 4.6) . This measurement was taken from solar cell of the structure (FTO/ ZnO / (Nile Blue with Chloroform) dye / Co₆₀ + Iodine /FTO), The short-circuit current (I_{sc}) is 18.77mA , the open-circuit voltage (V_{oc}) is 7.74mV, fill factor (FF) is 0.88, Density of current ($J_{sc}=3.0032\text{mA.cm}^{-2}$) and the efficiency is ($\eta=0.3719\%$). Fig (4.17) shows the current-voltage characteristics obtained from the measured values (see Table 4.7) . This measurement was taken from solar cell of the structure (FTO/ ZnO / (Nile Blue with Benzene) dye / Co₆₀ + Iodine /FTO), The short-circuit current (I_{sc}) is 17.55mA , the open-circuit voltage (V_{oc}) is 7.74mV, fill factor (FF) is 0.88 , Density of current ($J_{sc} =2.808 \text{ mA.cm}^{-2}$) and the efficiency is 0.3477%.

Table (4.8) Typical I-V riding of five sample that made by Blue Nile dye in different solvent (Methanol, Ethanol, Acton Chloroform and Benzene)

Sample	I_{sc} (mA)	I_m (mA)	V_m (mV)	V_{oc} (mV)	J_{sc} (mA.cm ⁻²)	FF	η %	Absor	E_g (eV)
B- Methanol	20.26	18.69	7.39	7.743	3.242	0.88	0.4017	2.006	3.276
B- Ethanol	19.85	18.55	7.34	7.72	3.176	0.89	0.3968	1.4819	3.272
B- Aceton	19.25	18.17	7.27	7.74	3.08	0.89	0.3858	1.221	3.269
B- Choroform	18.77	17.52	7.32	7.74	3.0032	0.88	0.3719	0.983	3.251
B- Benzeen	17.55	16.27	7.35	7.74	2.808	0.88	0.3477	0.532	3.246

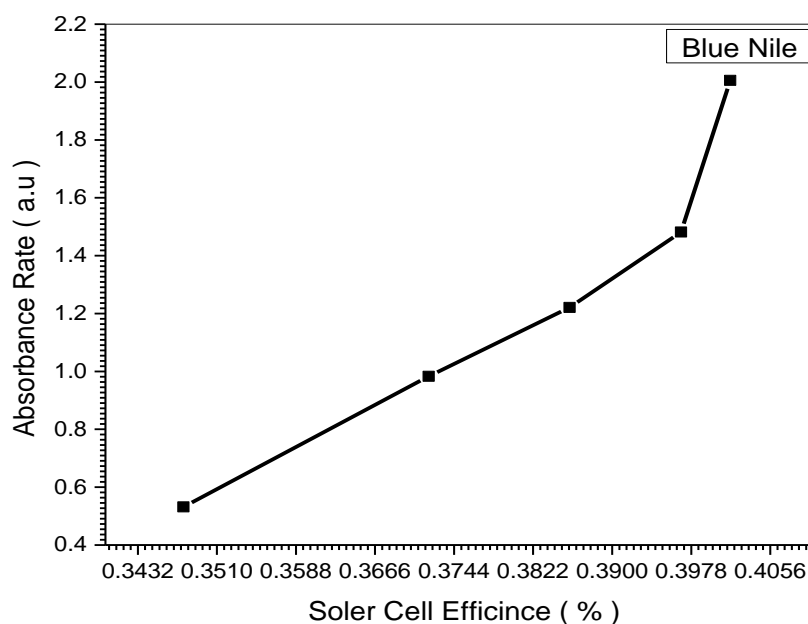


Figure 4.24 Absorbance and efficiency of Dye The relationship between Sensitized Solar Cells (DSSC) by (ZnO+ Nile Blue dye) samples.

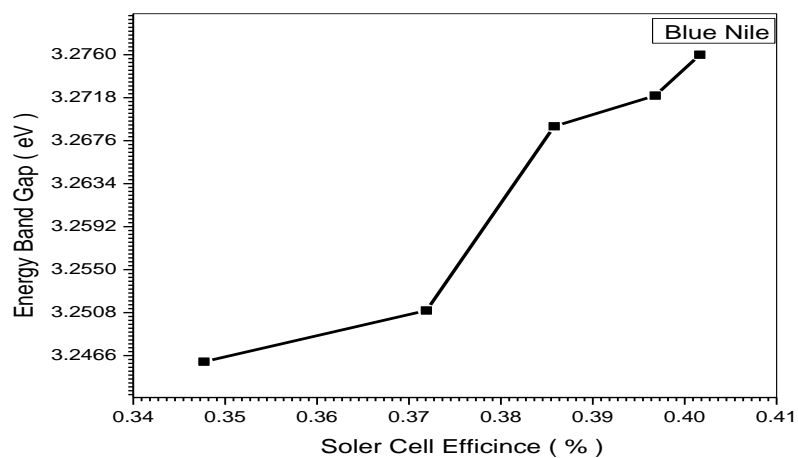


Figure 25 Relationship between energy band gap and efficiency of Dye Sensitized Solar Cells (DSSC) by (ZnO+ Nile Blue dye) samples

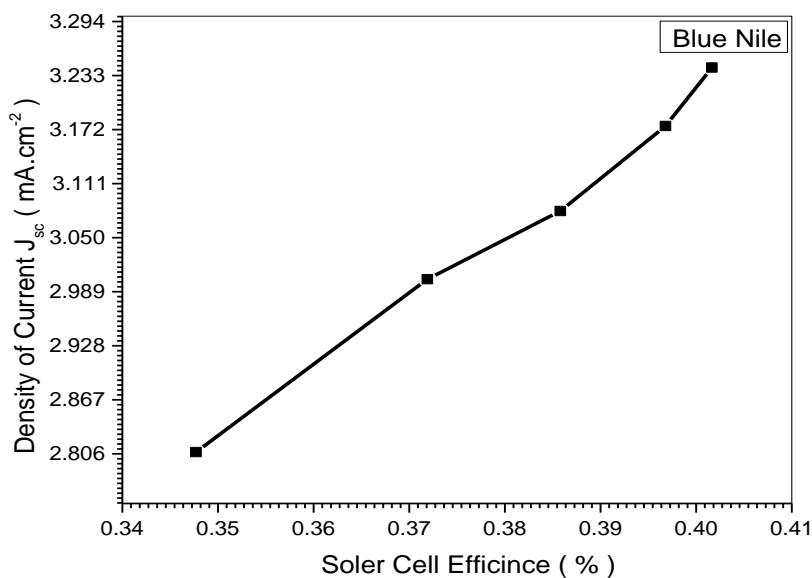


Figure 4.26 Relationship Between efficiency and Density of Dye Sensitized Solar Cells (DSSC) by (ZnO+ Nile Blue dye) samples

4.8 Dye Rose Bengal Results and Discussion

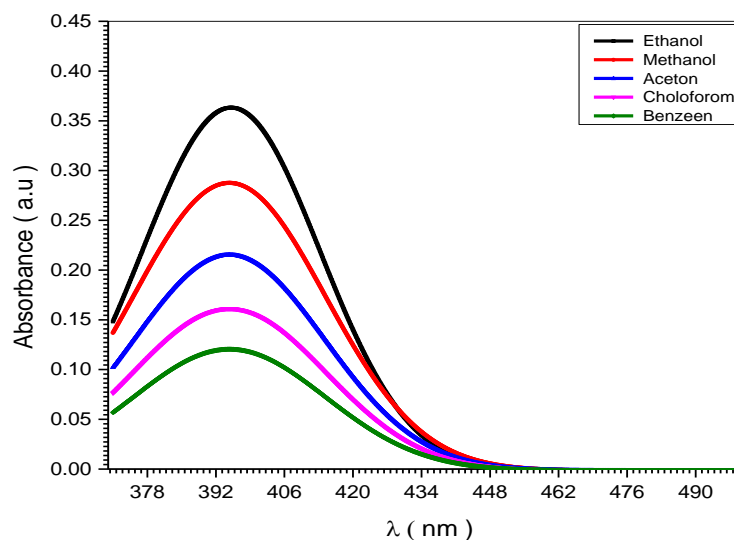


Figure 27 Relation between absorbance and wavelengths of five sample that made by Rose Bengal dye in different solvent (Methanol ,Ethanol ,Acton , Chloroform and Benzene)

In view of figures (4) and (28) the addition of the Rose Bengal and solvents changes the absorbance peak from about 330 nm and increase it to about 400 nm. This means that the solar cells enable to absorb more photons having wave length in the range of about 300- 400 nm. The energy gap decreases due to these addition from 0.3589eV to (2.947-2.972 eV) which enables more electrons to enter conduction band by longer photon wave lengths as indicated by figures (36) and (30).

Table (4.15) shows that the decrease of energy gap increase absorbance's and efficiencies as shown by figures (28) and (36) which shows that the increase of absorbance increase efficiency while the decrease of energy gap increase efficiencies. Both processes allows more electrons to be conduction band thus increase the efficiency as shown in figure (37).

It is very clear that the solvent type affect the energy gap table (4.9) shows that Methanol gives high efficiency followed by Ethanol,Acetone, Chloroform than Benzene which has low efficiency.

Table (9) Lattice Constants and Miller Indices [Cubic Face centered] of ZnO sample

Solvent	2-Theta	d(A°)	H	K	l	X _s (nm)
R- Methanol	17.943	2.67255	1	1	1	87.8
R- Ethanol	31.788	2.31450	2	0	0	47.8
R- Acetone	34.386	1.63660	2	2	0	53.8
R- chloroform	36.438	1.39570	3	1	1	48.8
R- Benzene	56.594	1.33628	2	2	2	62.3

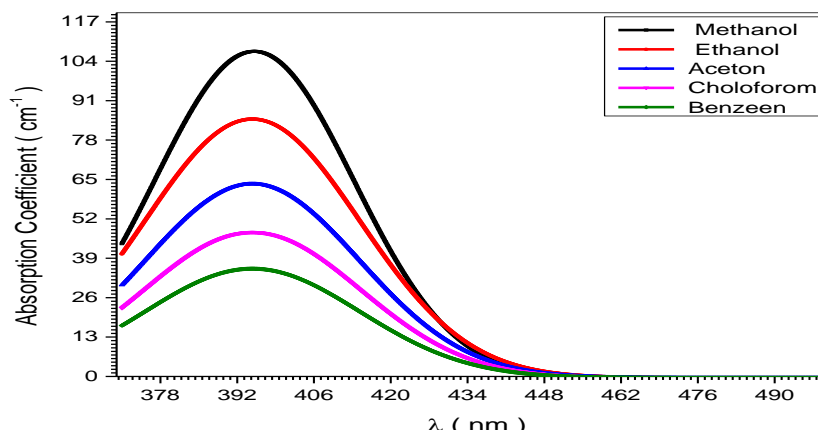


Figure 4.28 relation between absorption coefficient and wavelengths of five sample that made by Rose Bangal dye in different solvent (Methanol ,Ethanol ,Acton m Chloroform and Benzene)

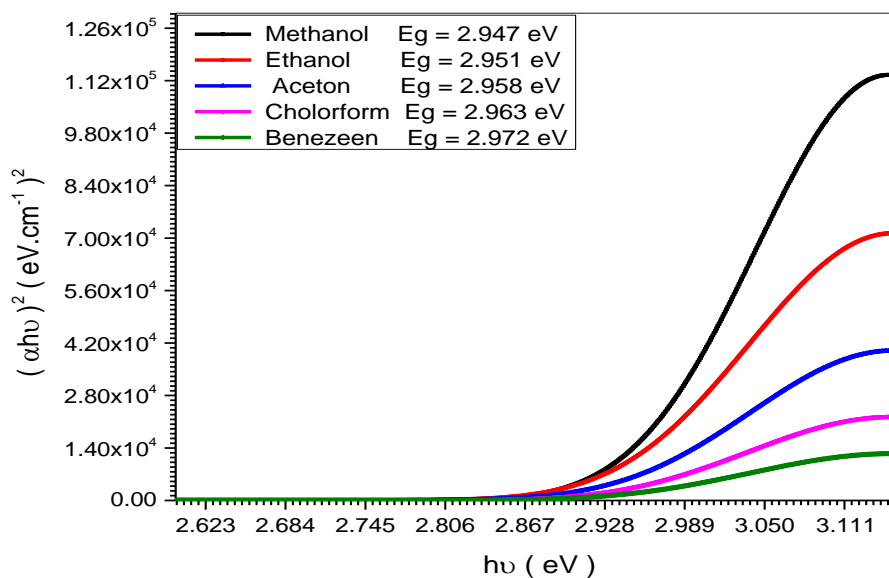


Fig4.29 The optical energy band gab of five sample that made by Rose Bengal dye in different solvent (Methanol ,Ethanol ,Acton m Chloroform and Benzene)

4.9 Rose Bengal Solar Cell Results and Discussion

Table 4.10 Typical I-V riding of Rose Bengal with Methanol solar cell

Voltage (mV)	Current (mA)
0	33.124
2.60709	33.64199
4.84015	33.97789
6.4569	33.97789
7.49956	26.18999
7.6663	13.92343
7.73	0

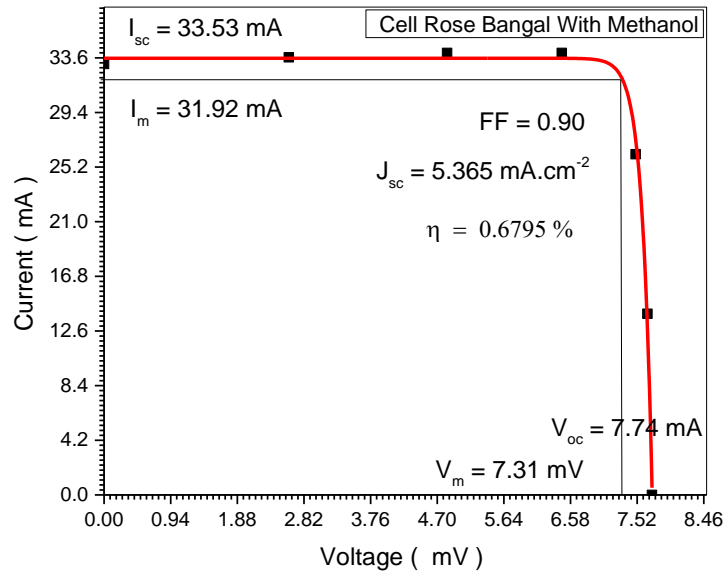


Figure 4.30 several factors for characterization of Rose Bengal with Methanol solar cell

Table 4.11 Typical I-V riding of Rose Bengal with Ethanol solar cell

Voltage (mV)	Current (mA)
0	31.4678
2.60709	31.95989
4.84015	32.27899
6.4569	32.27899
7.49956	24.88049
7.6663	13.22726
7.73	0

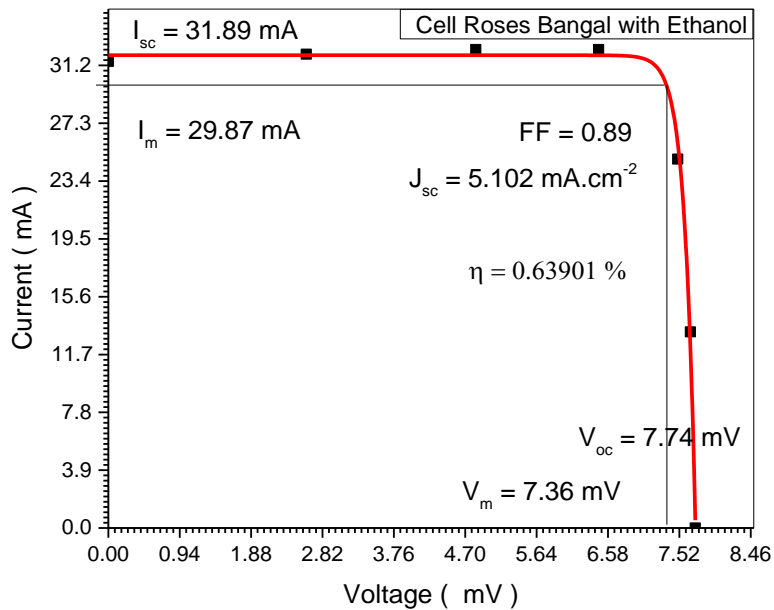


Figure 4.31 several factors for characterization of Rose Bangal with Ethanol solar cell

Table 4.12 Typical I-V riding of Rose Bangal with Acton solar cell

Voltage (mV)	Current (mA)
0	29.26505
2.60709	29.7227
4.84015	30.01946
6.4569	30.01946
7.49956	23.13886
7.6663	12.30135
7.73	0

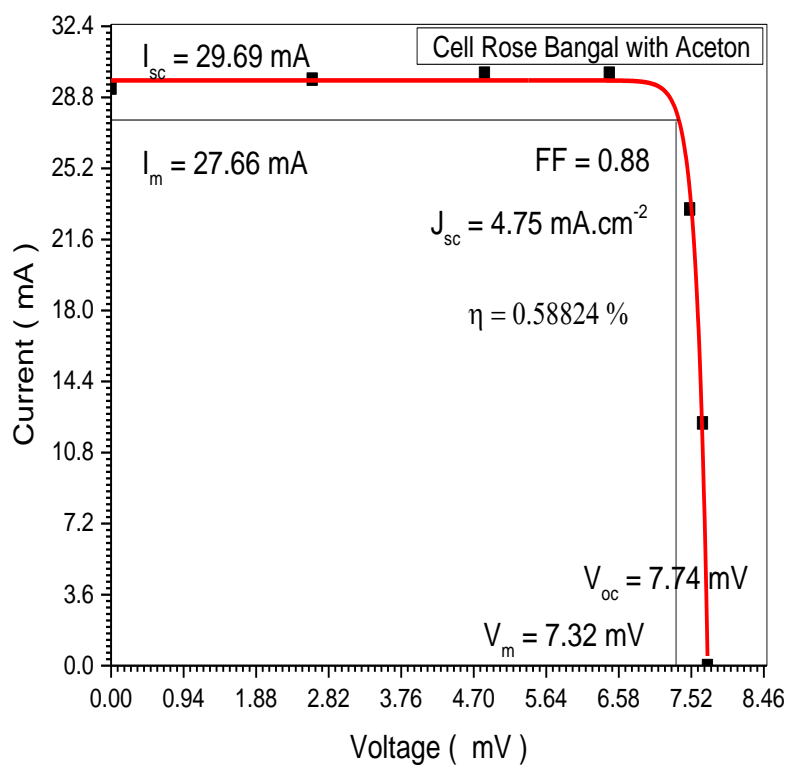


Figure 4.32 several factors for characterization of Rose Bengal with Acton solar cell

Table 4.13 Typical I-V riding of Rose Bengal with Chloroform solar cell

Voltage (mV)	Current (mA)
0	27.50915
2.60709	27.93933
4.84015	28.21829
6.4569	28.21829
7.49956	21.75053
7.6663	11.56327
7.73	0

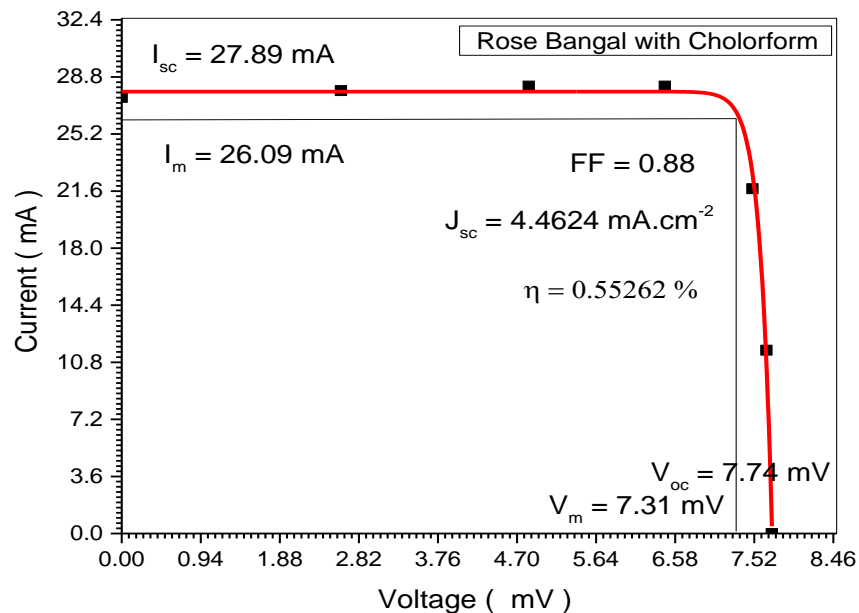


Figure 4.34 several factors for characterization of Rose Bangal with Chloroform solar cell

Table 4.14 Typical I-V riding of Rose Bangal with Benzene solar cell

Voltage (mV)	Current (mA)
0	25.30842
2.60709	25.70419
4.84015	25.96083
6.4569	25.96083
7.49956	20.01048
7.6663	10.63821
7.73	0

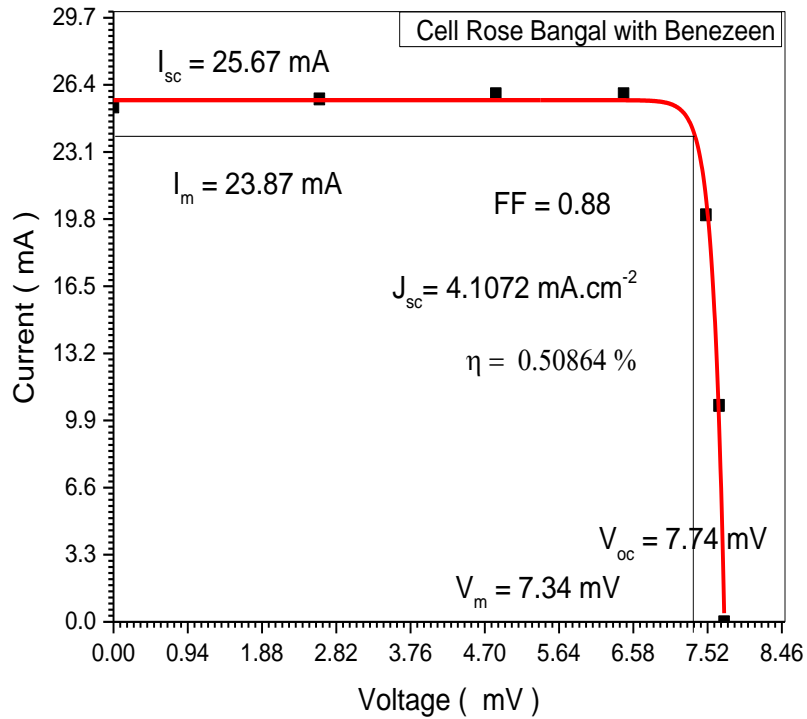


Figure 4.35 several factors for characterization of Rose Bangal with Benzene solar cell

Fig (4.15) shows the current-voltage characteristics obtained from the measured values (see Table 4.15) . This measurement was taken from solar cell of the structure (FTO/ ZnO / (Rose Bangal with Methanol) dye / Co₆₀ + Iodine /FTO), The short-circuit current (I_{sc}) is 33.53 mA , the open-circuit voltage (V_{oc}) is 7.74m V, fill factor (FF) is 0.90, Denisity of current ($J_{sc} = 5.365 \text{mA.cm}^{-2}$) and the efficiency is $\eta = 0.6795\%$. Fig(4.10) shows the current-voltage characteristics obtained from the measured values (see Table 4.11) . This measurement was taken from solar cell of the structure (FTO/ ZnO / (Rose Bangal with Ethanol) dye / Co₆₀ + Iodine /FTO), The short-circuit current (I_{sc}) is 31.89 mA , the open-circuit voltage (V_{oc}) is 7.74m V, fill factor (FF) is 0.89, Density of current ($J_{sc} =$

5.102 mA.cm⁻²) and the efficiency is $\eta=0.63901$.Fig(4.23) shows the current-voltage characteristics obtained from the measured values (see Table 4.12) . This measurement was taken from solar cell of the structure (FTO/ ZnO / (Rose Bangal with Acton) dye / Co₆₀ + Iodine /FTO), The short-circuit current (I_{sc}) is 29.69mA , the open-circuit voltage (V_{oc}) is 7.74mV, fill factor (FF) is 0.88, Density of current ($J_{sc} =4.75$ mA.cm⁻²) and the efficiency is ($\eta=0.58824\%$). Fig(4.24) shows the current-voltage characteristics obtained from the measured values (see Table 4.13) . This measurement was taken from solar cell of the structure (FTO/ ZnO / (Rose Bangal with Chloroform) dye / Co₆₀ + Iodine /FTO), The short-circuit current (I_{sc}) is 29.89mA, the open-circuit voltage (V_{oc}) is 7.74mV, fill factor (FF) is 0.88, Density of current ($J_{sc} =4.4624$ mA.cm⁻²) and the efficiency is $\eta=0.55262\%$. Fig (4.25) shows the current-voltage characteristics obtained from the measured values (see Table 4.14) . This measurement was taken from solar cell of the structure (FTO/ ZnO / (Rose Bangal with Benzene) dye / Co₆₀ + I+odine /FTO), The short-circuit current (I_{sc}) is 25.67mA , the open-circuit voltage (V_{oc}) is 7.74mV, fill factor (FF) is=0.88, Density of current ($J_{sc}=4.1072$ mA.cm⁻²) and the efficiency is ($\eta=0.50864\%$).

Table 4.15 Typical I-V riding of five sample that made by Rose Bangal dye in different solvent (Methanol ,Ethanol ,Acton m Chloroform and Benzene)

Sample	I_{sc} (mA)	I_m (mA)	V_m (mV)	V_{oc} (mV)	J (mA.cm ⁻²)	FF	η %	Absoe	E_g (eV)
R-Methanol	33.53	31.92	7.31	7.74	5.365	0.90	0.6795	0.366	2.947
R- Ethanol	31.89	29.87	7.36	7.74	5.102	0.89	0.63901	0.289	2.951
R- Acetone	29.69	27.66	7.32	7.74	4.75	0.88	0.58824	0.217	2.958
R- chloroform	27.89	26.09	7.31	7.74	4.4624	0.88	0.55262	0.162	2.963
R- Benzene	25.67	23.87	7.34	7.74	4.1072	0.88	0.50864	0.22	2.972

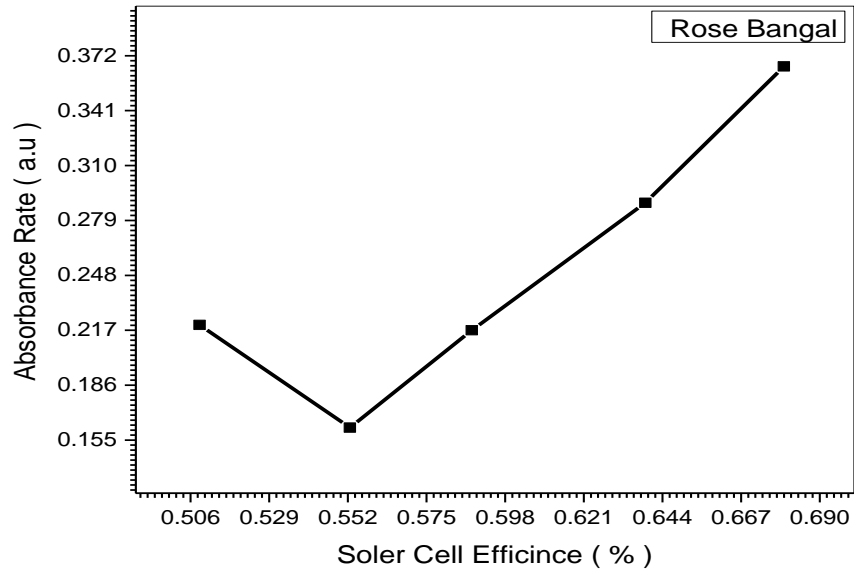


Figure 4.36 The relationship between Absorbance and efficiency of Dye Sensitized Solar Cells (DSSC) (ZnO+ Rose Bengal dye dye)samples

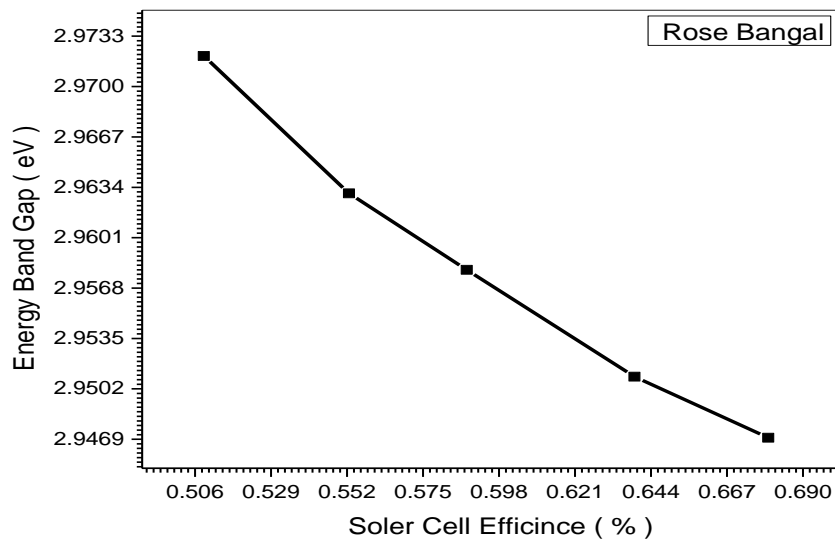


Figure 4.37 The relationship between Energy band gap and efficiency of Dye Sensitized Solar Cells (DSSC) (ZnO+ Rose Bengal dye dye) samples

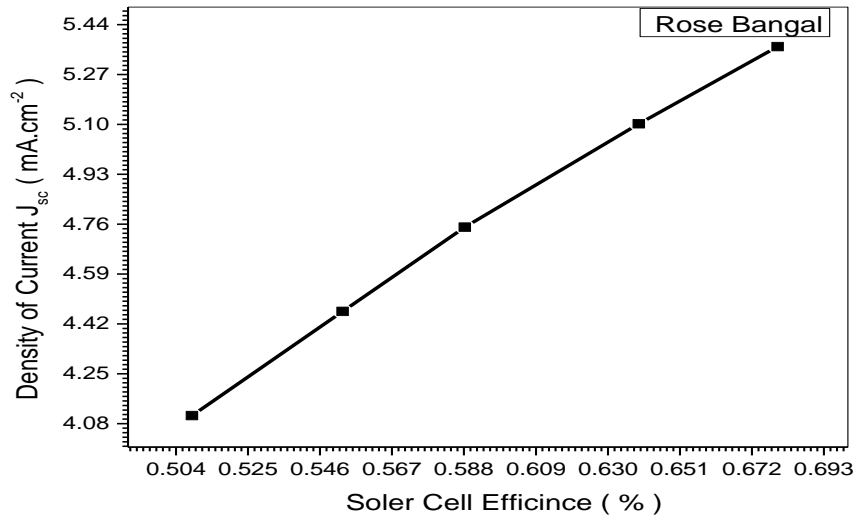


Figure 4.38 The relationship between Density Current and efficiency of Dye Sensitized Solar Cells (DSSC) (ZnO+ Rose Bengal dye dye) samples

Chapter Five

Conclusion and Recommendation

5.1 For Nile blue

The five sample of Dye Sensitized Solar Cells (DSSC) with Nile Blue were fabricated on FTO glass have a direct allow electronic transition with optical the value of the energy gap (E_g) of Blue Nile dye in different solvent (Methanol = 3.246 eV ,Ethanol = 3.251 eV ,Acton = 3.269 eV , Chloroform = 3.272 eV and Benzene = 3.276 eV) for all samples . The efficiency is (0.40165, 0.3968, 0.3858, 0.3719 and 0.3477)% for the current-voltage characteristics obtained from the measured values.

5.2 For Rose Bengal

When Rose Bengal dyes and some solvents are added to ZnO the solar cell efficiency and absorbance increase while the energy gap decreases. The solvent type affects clearly these parameters thus changing solar cell efficiency.

5.3 Recommendation

- Nano-materials infiltrate into human immune system and may cause problem.
- Increasing or decreasing of the temperature is a mean reason of ZnO formation defect.
- The impurity of nano-ZnO refer to the impuritized materials.
- Obtaining a maximum quantity of nano-ZnO from disposition process depend on substrate. research and development activities are currently ongoing

To facilitate the dissemination of Photovoltaic generation systems in the future, it is essential to develop and incorporate commonly-used fundamental

technologies and to reduce the cost of solar cells. For this purpose, the following

- Development of new solar cell evaluation technologies to increase the number of installations, methods to evaluate the performance and

Reliability of solar cell modules and solar generation systems are being developed.

- Development of Photovoltaic environmental technologies Studies are being conducted under a variety of environmental conditions and guidelines for Photovoltaic (PV) generation systems. The development of technology life-cycle assessment ies related to solar cell recycling and the development of (LCA) evaluation methods for PV generation are also being carried out.

- Study on Photovoltaic generation technology development trends research and development trends, future development direction and the analysis and evaluation of the state of PV generation aboard are being tracked.

5.4Future work

I more attention is required to other deposition techniques and to study the morphology of the resulting thin films. At the same time, if your primary interest is biology, the process of extracting photo pigments from different plants may also be investigated. The method used in this project can be repeated to improve purity or it can be halted at an early stage to include lots of different molecules, such as carotenoids and phycocobilins. Different sensitizers are also of interest, perhaps in conjunction with others, to improve the absorption spectrum. Another idea is to heat a dye-covered electrode, manufactured the standard way, at low temperature. This would perhaps allow for even better distribution

and absorption of the dye without damaging it, thus possibly increasing the efficiency of the solar cell.

Reference

- [1] Hochbaum A I and Yang P D 2010 Semiconductor nanowires for energy conversion *Chem. Rev.* 110 527-46.
- [2] Gregg B A 2003 Excitonic solar cells *J. Phys. Chem. B* 107 4688-98
- [3] Gledhill S E, Scott B and Gregg B A 2005 Organic and nano-structured composite photovoltaic: an overview *J. Mater. Res.* 20 3167-79
- [4] Coakley K M and McGehee M D 2004 Conjugated polymer photovoltaic cells *Chem. Mat.* 16 4533-42
- [5] Peumans P, Yakimov A and Forrest S R 2003 Small molecular weight organic thin-film photodetectors and solar cells *J. Appl. Phys.* 93 3693-723
- [6] Gratzel M 2000 Perspectives for dye-sensitized nanocrystalline solar cells *Prog. Photovoltaics* 8 171-85
- [7] Nazeeruddin M K, Kay A, Rodicio I, Humphrybaker R, Muller E, Liska P, Vlachopoulos N and Gratzel M 1993 Conversion of light to electricity by cis-X₂bis(2,2'-bipyridyl-4,4'-dicarboxylate)ruthenium(II) charge-transfer sensitizers (X = Cl⁻, Br⁻, I⁻, CN⁻, and SCN⁻) on nanocrystalline TiO₂ electrodes *J. Am. Chem. Soc.* 115 6382-90
- [8] Oregan B and Gratzel M 1991 A low-cost, high-efficiency solar-cell based on dye-sensitized colloidal TiO₂ films *Nature* 353 737-40
- [9] Gratzel M 2003 Dye-sensitized solar cells *J. Photochem. Photobiol. C-Photochem. Rev.* 4 145-53108
- [10] Sinke W C and Wienk M M 1998 Photochemistry - solid-state organic solar cells *Nature* 395 544-5

- [11] Bach U, Lupo D, Comte P, Moser J E, Weissortel F, Salbeck J, Spreitzer H and Gratzel M 1998 Solid-state dye-sensitized mesoporous TiO₂ solar cells with high photon-to-electron conversion efficiencies *Nature* 395 583-5
- [12] Kruger J, Plass R, Cevey L, Piccirelli M, Gratzel M and Bach U 2001 High efficiency solid-state photovoltaic device due to inhibition of interface charge recombination *Appl. Phys. Lett.* 79 2085-7
- [13] Lee T H, Sun D Z, Zhang X, Sue H J and Cheng X 2009 Solid-state dye-sensitized solar cell based on semiconducting nanomaterials *J. Vac. Sci. Technol. B* 27 3073-7
- [14] Schmidt-Mende L, Zakeeruddin S M and Gratzel M 2005 Efficiency improvement in solid-state-dye-sensitized photovoltaics with an amphiphilic ruthenium-dye *Appl. Phys. Lett.* 86 013504
- [15] Li G, Shrotriya V, Huang J S, Yao Y, Moriarty T, Emery K and Yang Y 2005 High-efficiency solution processable polymer photovoltaic cells by self-organization of polymer blends *Nat. Mater.* 4 864-8
- [16] Padinger F, Rittberger R S and Sariciftci N S 2003 Effects of postproduction treatment on plastic solar cells *Adv. Funct. Mater.* 13 85-8
- [17] Reyes-Reyes M, Kim K and Carroll D L 2005 High-efficiency photovoltaic devices based on annealed poly(3-hexylthiophene) and 109-(31)-methoxycarbonyl)-propyl-1-phenyl-(6,6)C₆₁ blends *Appl. Phys. Lett.* 87 083506
- [18] Liang Y Y, Xu Z, Xia J B, Tsai S T, Wu Y, Li G, Ray C and Yu L P 2010 For the bright future-bulk heterojunction polymer solar cells with power conversion efficiency of 7.4% *Adv. Mater.* 22 E135-8
- [19] Beek W J E, Wienk M M and Janssen R A J 2004 Efficient hybrid solar cells from zinc oxide nanoparticles and a conjugated polymer *Adv. Mater.* 16 1009-13

- [20] Yadav, A. and Kumar, P. (2015) Enhancement in Efficiency of PV Cell through P&O Algorithm. International Journal for Technological Research in Engineering, **2**, 2642-2644.
- [21] Castellano, R. (2010) Solar Panel Processing. Old City Publishing Inc., Philadelphia.
- [22] Srinivas, B., Balaji, S., Nagendra Babu, M. and Reddy, Y.S. (2015) Review on Present and Advance Materials for SolarCells. International Journal of Engineering Research-Online, **3**, 178-182.
- [23] McEvoy, A., Castaner, L. and Markvart, T. (2012) Solar Cells: Materials, Manufacture and Operation. 2nd Edition, Elsevier Ltd., Oxford, 3-25.
- [24] Grisham, L.R. (2008) Nuclear Fusion in: Future Energy, Improved, Sustainable and Clean Options for our Planet, Edited by Trevor M. Letcher, 2nd Edition, Elsevier Ltd., Amsterdam, 291-301.
- [25] Fahrenbruch, A.L. and Bube, R.H. (1983) Fundamentals of Solar Cells. Academic Press Inc., New York.
- [26] McEvoy, A., Castaner, L. and Markvart, T. (2012) Solar Cells: Materials, Manufacture and Operation. 2nd Edition, Elsevier Ltd., Oxford, 3-25.
- [27] Bertolli, M. (2008) Solar Cell Materials. Course: Solid State II. Department of Physics, University of Tennessee, Knoxville
- [28] Bagher, A.M., Vahid, M.M.A. and Mohsen, M. (2015) Types of Solar Cells and Application. American Journal of Optics and Photonics, **3**, 94-113. [29] Choubey, P.C., Oudhia, A. and Dewangan, R. (2012) A Review: Solar Cell Current Scenario and Future Trends. Recent Research in Science and Technology, **4**, 99-101.

- [30] Fahrenbruch, A.L. and Bube, R.H. (1983) Fundamentals of Solar Cells. Academic Press Inc., New York.
- [31] Bagher, A.M., Vahid, M.M.A. and Mohsen, M. (2015) Types of Solar Cells and Application. American Journal of Optics and Photonics, 3, 94-113.
- [32] Srinivas, B., Balaji, S., Nagendra Babu, M. and Reddy, Y.S. (2015) Review on Present and Advance Materials for Solar Cells. International Journal of Engineering Research-Online, 3, 178-182.
- [33] Chopra, K.L., Paulson, P.D. and Dutt, V. (2004) Thin-Film Solar Cells: An Overview. Progress in Photovoltaics, 12, 69-92. <http://dx.doi.org/10.1002/pip.541>
- [34] Srinivas, B., Balaji, S., Nagendra Babu, M. and Reddy, Y.S. (2015) Review on Present and Advance Materials for Solar Cells. International Journal of Engineering Research-Online, 3, 178-182.
- [35] Choubey, P.C., Oudhia, A. and Dewangan, R. (2012) A Review: Solar Cell Current Scenario and Future Trends. Recent Research in Science and Technology, 4, 99-101.
- [36] Nozik, A.J. (2010) Nanoscience and Nanostructures for Photovoltaics and Solar Fuels. NANO Letters, 10, 2735-2741. <http://dx.doi.org/10.1021/nl102122x>
- [37] Barnes, P.R.F., Anderson, A.Y., Koops, S.E., Durrant, J.R. and O'Regan, B.C. (2009) Electron Injection Efficiency and Diffusion Length in Dyesensitized Solar Cells Derived from Incident Photon Conversion Efficiency Measurements. The Journal of Physical Chemistry C, 113, 1126-1136. <http://dx.doi.org/10.1021/jp809046j>
- [38] Philipps, S.P., Bett, A.W., Horowitz, K. and Kurtz, S. (2015) Current Status of Concentrator Photovoltaics (CPV) Technology. Report Version 1.2, Fraunhofer Institute for Solar Energy Systems (NREL), September 2015.

- [39] Bertolli, M. (2008) Solar Cell Materials. Course: Solid State II. Department of Physics, University of Tennessee, Knoxville.
- [40] Philipps, S.P., Bett, A.W., Horowitz, K. and Kurtz, S. (2015) Current Status of Concentrator Photovoltaics (CPV) Technology. Report Version 1.2, Fraunhofer Institute for Solar Energy Systems (NREL), September 2015.
- [41] Mohanta, P. R., Patel, J., Bhuvra, J. and Gandhi, M. (2015) A Review on Solar Photovoltaics and Roof Top Application of It. International Journal of Advanced Research in Science, Engineering and Technology, **2**, 2394-2444.
- [42] Philipps, S.P., Bett, A.W., Horowitz, K. and Kurtz, S. (2015) Current Status of Concentrator Photovoltaics (CPV) Technology. Report Version 1.2, Fraunhofer Institute for Solar Energy Systems (NREL), September 2015.
- [43] M. Ejder, R.T. Carlsen, Cost drivers in the photovoltaic solar industry. KTH – School of Industrial Engineering and Management, Stockholm (SE) (2011). (Bachelorthesis) <http://urn.kb.se/resolve?urn=urn:nbn:se:kth:diva-58790>
- [44] M. Kerstens, Solexel unveils ultra-thin, high-performance silicon solar cell at inter solar. Pressrelease (2012). http://www.Appliednanotech.net/news/Solexel_p
- [45] Li, B., Wang, L., Kang, B., Wang, P. and Qiu, Y. (2006) Review of Recent Progress in Solid-State Dye-Sensitized Solar Cells. Solar Energy Materials and Solar Cells, **90**, 549-573. <http://dx.doi.org/10.1016/j.solmat.2005.04.039> [46] Nozik, A.J. (2010) Nanoscience and Nanostructures for Photovoltaics and Solar Fuels. NANO Letters, **10**, 2735-2741. <http://dx.doi.org/10.1021/nl102122x> [47] Bagher, A.M., Vahid, M.M.A. and Mohsen, M. (2015) Types of Solar Cells and Application. American Journal of Optics and Photonics, **3**, 94-113.

- [48] Srinivas, B., Balaji, S., Nagendra Babu, M. and Reddy, Y.S. (2015) Review on Present and Advance Materials for Solar Cells. International Journal of Engineering Research-Online, **3**, 178-182.
- [49] Suhaimi, S., Shahimin, M.M., Alahmed, Z.A., Chyský, J. and Reshak, A.H. (2015) Materials for Enhanced Dye-Sensitized Solar Cell Performance: Electrochemical Application. International Journal of Electrochemical Science, **10**, 28-59.
- [50] Graetzel, M., Janssen, R.A.J., Mitzi, D.B. and Sargent, E.H. (2012) Materials Interface Engineering for Solution- Processed Photovoltaics. Nature, **488**, 304-312. <http://dx.doi.org/10.1038/nature11476>
- [51] Suhaimi, S., Shahimin, M.M., Alahmed, Z.A., Chyský, J. and Reshak, A.H. (2015) Materials for Enhanced Dye-Sensitized Solar Cell Performance: Electrochemical Application. International Journal of Electrochemical Science, **10**, 28-59.
- [52] Liang, M., Xu, W., Cai, F.S., Chen, P.Q., Peng, B., Chen, J. and Li, Z.M. (2007) New Triphenylamine-Based Organic Dyes for Efficient Dye-Sensitized Solar Cells. The Journal of Physical Chemistry C, **111**, 4465-4472. <http://dx.doi.org/10.1021/jp067930a>.
- [53] Bertolli, M. (2008) Solar Cell Materials. Course: Solid State II. Department of Physics, University of Tennessee, Knoxville.
- [54] Bykov, VP. Soviet Physics JETP, American Institute of Physics, 197235, 269.
- [55] Goetzberger, A; Goldschmidt, JC; Peters, M; Löper, P. Sol En Mat Sol Cells, 2008, 92, 1570–1578.
- [56] Löper, P. et al. Proceedings of the 23rd European Photovoltaic Solar Energy Conference 2008.

- [57] Johnson, SD; Joannopoulos, SD. Opt Exp.2001, 8, 173-190. Keil, G. J. Appl Phys.1969, 40,3544. [58] K. Okada, H. Matsui, T. Kawashima, T. Ezure, N. Tanabe, Journal of Photochemistry & Photobiology, A: Chemistry 164/1-3 (2004) 193.
- [59] B.D. Cullity, Elements of X-ray Diffraction 2ndEd. (Addison-Wesley, Reading, MA, 1978)
- [60] .W. Vallejo, J. Clavijo, Brazilian Journal of Physics, 40 (2010) 30.
- [61] .[Subba Ramaiah, K.; Sundara Raja, V. Structural and electrical properties of fluorine doped tin oxide films prepared by spray-pyrolysis technique. Appl. Surf. Sci. 2006, 253, 1451–1458.
- [62].Tefamichael, T.; Will, G.; Colella, M.; Bell, J. Optical and electrical properties of nitrogen ion implanted fluorine doped tin oxide films. Nucl. Instrum. Methods Phys. Res. B Beam Interact. Mater. Atoms 2003, 201, 581–588.
- [63].Kim, C.-Y.; Riu, D.-H. Texture control of fluorine-doped tin oxide thin film. Thin Solid Films 2011, 519, 3081–3085.
- [64].Gerhardinger, P.F.; McCurdy, R.J. Float line deposited transparent conductors—Implications for the PV industry.MRSProc.1996, 426, 399–410.
- [65].Sankara Subramanian, N.; Santhi, B.; Sundareswaran, S.; Venkatakrishnan, K.S. Studies on spray deposited SnO₂, Pd:SnO₂ and F:SnO₂ thin films for gas sensor applications. Synth. React. Inorg. Metal-Organic Nano-Metal Chem. 2006, 36, 131–135. [66].Yadav, A.A.; Masumdar, E.U.; Moholkar, A.V.; NmannSpallart, M.; Rajpure, K.Y.; Bhosale, C.H. Electrical, structural and optical properties of SnO₂:F thin films: Effect of the substrate temperature. J. Alloy. Compd. 2009, 488, 350–355.

- [67].Sheel, D.W.; Gaskell, J.M. Deposition of fluorine doped indium oxide by atmospheric pressure chemical vapour deposition. *Thin Solid Films* 2011, 520, 1242–1245. [68].Kim, H.; Auyeung, R.C.Y.; Piqué, A. Transparent conducting F-doped SnO₂ thin films grown by pulsed laser deposition. *Thin Solid Films* 2008, 516, 5052–5056.
- [69].Mientus, R.; Ellmer, K. Structural, electrical and optical properties of SnO₂–X:F-layers deposited by DC-reactive magnetron sputtering from a metallic target in Ar–O₂/CF₄ mixtures. *Surf. Coat. Technol.* 1998, 98, 1267–1271. *Coatings* 20144 745
- [70].Elangovan, E.; Ramamurthi, K. Studies on micro-structural and electrical properties of spray-deposited fluorine-doped tin oxide thin films from low-cost precursor. *Thin Solid Films* 2005, 476, 231236.
- [71].Gorley, P.M.; Khoyak, V.V.; Bilichuk, S.V.; Oletsky, I.G.; Horley, P.P.; Grechko, V.O. SnO₂ films: Formation, electrical and optical properties. *Mater. Sci. Eng. B* 2005, 118, 160–163.
- [72].Maruyama, T.; Akagi, H. Fluorine-doped tin dioxide thin films prepared by radio-frequency magnetron sputtering. *J. Electrochem. Soc.* 1996, 143, 283–287.
- [73].Čada, M.; Bradley, J.W.; Clarke, G.C.B.; Kelly, P.J. Measurement of energy transfer at an isolated substrate in a pulsed dc magnetron discharge. *J. Appl. Phys.* 2007, 102, doi:10.1063/1.2779287.
- [74] Baruah, S. and Dutta, J.; Dutta (2009). "Hydrothermal growth of ZnO nanostructures". *Sci. Technol. Adv. Mater.* (free download pdf) **10**: 013001. Bibcode:2009STAdM..10a3001B. doi:10.1088/14686996/10/1/013001.
- [75] Miao, L.; Ieda, Y.; Tanemura, S.; Cao, Y.G.; Tanemura, M.; Hayashi, Y.; Toh, S.; Kaneko, K. (2007). "Synthesis, microstructure and photoluminescence

of well-aligned ZnO nanorods on Si substrate". *Science and Technology of Advanced Materials* (free download pdf) **8** (6):443. Bibcode:2007STAdM...8..443M. doi:10.1016/j.stam.2007.02.012.

[76] Xu, S.; Wang, ZL. (2011). "One-dimensional ZnO nanostructures: Solution growth and functional properties". *Nano Res.* **4** (11): 1013–1098. doi:10.1007/s12274-011-0160-7.

[77] Ying Zhou et al. (2008). "Hydrothermal synthesis of ZnO nanorod arrays with the addition of polyethyleneimine". *Materials Research Bulletin* **43** (8–9): 2113–2118. doi:10.1016/j.materresbull.2007.09.024.

[78] -Cui, Jingbiao et al. (2006). "Synthesis and magnetic properties of Co-doped ZnO nanowires". *Journal of Applied Physics* **99** (8): 08M113. Bibcode:2006JAP....99hM113C. doi:10.1063/1.2169411.

[79] Elen, K. et al. (2009). "Hydrothermal synthesis of ZnO nanorods: a statistical determination of the significant parameters in view of reducing the diameter". *Nanotechnology* **20**(5):055608. Bibcode:2009Nanot..20e5608E. doi: 10.1088/0957-4484/20/5/055608. PMID 19417355.

[80].Greene; L. E. et al. (2003). "Low-Temperature Wafer-Scale Production of ZnO Nanowire Arrays". *Angew. Chem. Int. Ed* **42** (26): 3031–3032. doi:10.1002/anie.200351461. PMID 12851963.

[81] Wu, Wan-Yu et al. (2009). "Effects of Seed Layer Characteristics on the Synthesis of ZnO Nanowires". *Journal of the American Ceramic Society* **92** (11): 2718–2723. doi:10.1111/j.1551-2916.2009.03022.x.

[82] Greene, L. E.; Law, M; Tan, DH; Montano, M; Goldberger, J; Somorjai, G; Yang, P (2005). "General Route to Vertical ZnO Nanowire Arrays Using

Textured ZnO Seeds". *Nano Letters* **5** (7): 1231–1236.
Bibcode:2005NanoL...5.1231G.doi:10.1021/nl050788p.PMID 16178216.

[83] Hua, Guomin et al. (2008). "Fabrication of ZnO nanowire arrays by cycle growth in surfactantless aqueous solution and their applications on dye-sensitized solar cells". *Materials Letters* **62** (25): 4109–4111. doi:10.1016/j.matlet.2008.06.018.

[84] Lee, J.-H. et al. (2009). "Density-controlled growth and field emission property of aligned ZnO nanorod arrays". *Appl Phys A* **97** (2): 403–408. Bibcode:2009ApPhA..97..403L. doi:10.1007/s00339-009-5226-y.

[85] Özgür, Ü.; Alivov, Ya. I.; Liu, C.; Teke, A.; Reshchikov, M. A.; Doğan, S.; Avrutin, V.; Cho, S.-J.; Morkoç, H. (2005). "A comprehensive review of ZnO materials and devices". *Journal of Applied Physics* **98** (4): 041301. Bibcode:2005JAP....98d1301O. doi:10.1063/1.1992666.

[86] Look, D.C.; Hemsley, J.W.; Sizelove, J.R. (1999). "Residual Native Shallow Donor in ZnO". *Physical Review Letters* **82** (12): 2552. Bibcode:1999PhRvL..82.2552L. doi:10.1103/PhysRevLett.82.2552.

[87] Janotti, A. and Van De Walle, C.G.; Van De Walle (2007). "Hydrogen multicentre bonds". *Nature Materials* **6** (1): 44–7. Bibcode:2007NatMa...6...44J. doi:10.1038/nmat1795. PMID 17143265.

[88] K. Okada, H. Matsui, T. Kawashima, T. Ezure, N. Tanabe, *Journal of Photochemistry & Photobiology, A: Chemistry* 164/1-3 (2004) 193.

[89] A. K. Ray, S. M. Tracey, and S. N. B. Hodgson, *J. Phys. D* 36, 1409 (2003).

[90]. Sathyanarayana P, R. B. (2015). Effect of Shading on the Performance of Solar PV Panel. *Energy and Power*.

- [91]. Sofyan A. Taya¹, *. T.-A.-G.-L. (2013). Dye-sensitized solar cells using fresh and dried natural. *International Journal of Materials Science and Applications*.
- [92]. Sujata Saxena, A. S. (2004). *Natural Dyes: Sources, Chemistry, natural*.
- [93]. A. DUMBRAVĂa, A. G. (2008). Dye-sensitized solar cells based on nanocrystalline. *Journal Of Optoelectronics And Advanced Materials*. [94] [△] Ludvíková, Lucie; Friš, Pavel; Heger, Dominik; Šebej, Peter; Wirz, Jakob; Klán, Petr (2016). "Photochemistry of rose bengal in water and acetonitrile: a comprehensive kinetic analysis". *Physical Chemistry Chemical Physics*. **18** (24): 16266–16273. doi:10.1039/C6CP01710J. ISSN 1463-9076.
- [95] [^] Jump up to: ^a ^b ^c Jose, Jiney; Burgess, Kevin (2006). "Benzophenoxazine-based fluorescent dyes for labeling biomolecules" (PDF). *Tetrahedron*. **62** (48): 11021. doi:10.1016/j.tet.2006.08.056.
- [96]. Torrance, J.B.; Lacorre, P.; Asavaroengchai, C.; Metzger, R.M. Why are some oxides metallic, while most are insulating? *Physica C* **1991**, 182, 351–364.
- [97]. Chopra, K.; Major, S.; Pandya, D. Transparent conductors—A status review. *Thin Solid Films* **1983**, 102, 1–46.
- [98]. Zhai, T.; Fang, X.; Liao, M.; Xu, X.; Zeng, H.; Yoshio, B.; Golberg, D. A comprehensive review of one-dimensional metal-oxide nanostructure photodetectors. *Sensors* **2009**, 9, 6504–6529.
- [99]. Robertson, J. High dielectric constant gate oxides for metal oxide Si transistors. *Rep. Prog. Phys.* **2006**, 69, 327–396.
- [100]. Gellings, P.; Bouwmeester, H. Ion and mixed conducting oxides as catalysts. *Catal. Today* **1992**, 12, 1–105.

- [101]. Bocquet, A.; Mizokawa, T.; Morikawa, K.; Fujimori, A.; Barman, S.; Maiti, K.; Sarma, D.; Tokura, Y.; Onoda, M. Electronic structure of early 3d-transition-metal oxides by analysis of the 2p core-level photoemission spectra. *Phys. Rev. B* **1996**, 53, 1161–1170.
- [102]. Cardelli, F. *Materials Handbook: A Consise Desktop Reference*, 2nd ed.; Springer-Verlag: Hamburg, Germany, 2008.
- [103]. Yin, W.J.; Wei, S.H.; Al-Jassim, M.M.; Yan, Y. Prediction of the chemical trends of oxygen vacancy levels in binary metal oxides. *Appl. Phys. Lett.* **2011**, 99, 142109:1–142109:3.
- [104]. Meyer, B.K.; Polity, A.; Reppin, D.; Becker, M.; Hering, P.; Klar, P.J.; Sander, T.; Reindl, C.; Benz, J.; Eickhoff, M.; et al. Binary copper oxide semiconductors: From materials towards devices. *Phys. Stat. Solidi B* **2012**, 249, 1487–1509.
- [105]. Chen, L.C. Review of preparation and optoelectronic characteristics of Cu₂O-based solar cells with nanostructure. *Mater. Sci. Semincond. Process.* **2013**, 16, 1172–1185.
- [106]. Minami, T.; Miyata, T.; Nishi, Y. Efficiency improvement of Cu₂O-based heterojunction solar cells fabricated using thermally oxidized copper sheets. *Thin Solid Films* **2013**, in press.
- [107]. Freeman, A.; Poepelmeier, K.; Mason, T.; Chang, R.; Marks, T. Chemical and thin film strategies for new transparent conducting oxides. *MRS Bull.* **2000**, 25, 45–51.
- [108]. Kawazoe, H.; Yasukawa, M.; Hyodo, H.; Kurita, M.; Yanagi, H.; Hosono, H. P-type electrical conduction in transparent thin films of CuAlO₂. *Nature* **1997**, 389, 939–942.

- [109]. Kawazoe, H.; Yanagi, H.; Ueda, K.; Hosono, H. Transparent p-type conducting oxides: Design and fabrication of p-n heterojunctions. *MRS Bull.* **2000**, *25*, 28–36. *Coatings* **2014**, *4* **192** .
- [110]. Ögzur, Ü.; Alivov, Y.I.; Liu, C.; Teke, A.; Reshchikov, M.; Dogan, S.; Avrutin, V.; Cho, S.J.; Morkoç, H. A comprehensive review of ZnO materials and devices. *J. Appl. Phys.* **2005**, *98*, doi:10.1063/1.1992666.
- [111]. Van de Walle, C. Hydrogen as a cause of doping in zinc oxide. *Phys. Rev. Lett.* **2000**, *85*, 1012–1015.
- [112]. Ögzur, Ü.; Alivov, Y.I.; Liu, C.; Teke, A.; Reshchikov, M.; Dogan, S.; Avrutin, V.; Cho, S.J.; Morkoç, H. A comprehensive review of ZnO materials and devices. *J. Appl. Phys.* **2005**, *98*, doi:10.1063/1.1992666.
- [113]. Stirn, R.J.; Yeh, Y.C.M. A 15% efficient antireflection-coated metal-oxide-semiconductor solar cell. *Appl. Phys. Lett.* **1975**, *27*, 95–98.
- [114]. World Record Solar Cell with 44.7% Efficiency. Press Release 2013. Fraunhofer-Institut für Solare Energiesysteme ISE: Freiburg im Breisgau, Germany, 23 September 2013. Available online: <http://www.ise.fraunhofer.de/en/press-and-media/press-releases/presseinformationen-2013/world-record-solar-cell-with-44.7-efficiency> (accessed on 17 March 2014).
- [115]. Matthews, I., O'Mahony, D., Corbett, B., Morrison, A.P.: Theoretical performance of multijunction solar cells combining III-V and Si materials. *Opt. Express* *20*, 5 (2012)
- [116]. Kurtz, S., Meyers, D., McMahon, W.E., Geisz, J., Steiner, M.: A comparison of theoretical efficiencies of multijunction concentrator solar cells. *Prog. Photovolt. Res. Appl.* *16*, 6 (2008)

- [117]. King, R., et al.: 40% efficient metamorphic GaInP/GaInAs/Ge multijunction solar cells. *Appl. Phys. Lett.* 90, 183516 (2007)
- [118]. Tobias, I., Luque, A.: Ideal efficiency of monolithic, series-connected multijunction solar cells. *Prog. Photovolt. Res. Appl.* 10, 323–329 (2002)
- [119] M. A. Green, *Prog Photovoltaics Res Appl* **9**, 123 (2001).
- [120]. Jorgesen, M., Norrman, K., Gevorgyan, S.A., Tromholt, T., Andreasen, B., Krebs, F.C.: Stability of polymer solar cells. *Adv. Mater.* 24, 580–612 (2012)
- [121]. Arici, E., Sariciftci, N., Serdar, N., Dieter, M.: *Encyclopedia of Nanoscience and Nanotechnology*, vol. 3, pp. 99–944. (2004). [122] J. Nelson, *The Physics of Solar Cells* (Imperial College Press, 2003).
- [123] L. M. Peter, *Phys. Chem. Chem. Phys.* **9**, 2630 (2007).
- [124] J. Nelson, *The Physics of Solar Cells* (Imperial College Press, 2003).